Effects of mechanical measures and urban morphology on pollutant dispersion in urban areas: A review

Zhengtong Li [c], Tingzhen Ming [a,b,*], Shurong Liu [a], Chong Peng [d], Renaud de Richter [e], Wei Li [f], Hao Zhang [c], Chih-Yung Wen [c]

a. School of Civil Engineering and Architecture, Wuhan University of Technology, Wuhan 430070, China

b. School of Architectural Engineering, Huanggang Normal University, No. 146 Xingang Second Road, Huanggang 438000 China.

c. Department of Mechanical Engineering and Interdisciplinary Division of Aeronautical and Aviation Engineering, The Hong Kong Polytechnic University, Kowloon, Hong Kong

d. School of Urban Planning and Architecture, Huazhong University of Science and Technology, Wuhan 430074, China

e. Tour-Solaire.Fr, 8 Impasse des Papillons, F34090 Montpellier, France

f. European Bioenergy Research Institute, Aston Institute of Materials Research, Aston University, Birmingham, UK.

∗ corresponding author

Tingzhen Ming, Professor, School of Civil Engineering and Architecture, Wuhan University of Technology, Wuhan 430070, China

Email: tzming@whut.edu.cn

ABSTRACT:

Cities are facing significant challenges due to low outdoor air quality. Hence, a growing number of studies have been conducted to develop strategies for improving air quality. This paper provides a comprehensive and systematic review of the mechanisms and effects of various mechanical measures and urban morphology on pollutant dispersion in an urban context. Moreover, a detailed quantification of the reduction potential of the mechanical measures and urban morphology is provided, followed by the identification of the critical urban factors for the practical urban optimizing strategies. Additionally, the two fundamental processes (mean flow and turbulence) affecting the pollutant dispersion are clarified to understand the dilution mechanism of pollutants. For these purposes, the reviewed papers are categorized into two groups:

(i) Utilizing mechanical measures

(ii) Designing appropriate urban morphology

Generally, this study is useful for urban planners and architects who are responsible for decision-making.

Keywords: Air quality; Pollutant mitigations; Mechanical factors; Urban morphology; Local mitigation strategies;

1. Introduction

Ongoing global urbanization and high traffic emissions have resulted in numerous climatic and environmental problems [1,2], hence significantly affecting public health (e.g., respiratory and lung diseases) [3] and even causing great economic loss [4]. Annually, nearly 3 million people have died prematurely due to increasingly deteriorated air quality worldwide [5]. These deaths have been attributed to the significant increase in the demand for private motor vehicles because of substantial population growth [6], causing very high concentrations of air pollutants [7]. More importantly, in cities experiencing rapid development with intensive infrastructure construction, pollutant dispersion as a significant mitigation measure for airborne pollution is not commonly considered [7]. Accordingly, hasty and irrational construction strategies led to a lack of ventilation, preventing pollutant dispersion [8]. Therefore, it is essential to obtain an in-depth understanding of the pollutant dispersion mechanism in urban areas.

Deteriorating outdoor air quality worldwide has caused an increasing interest of researchers. There has been a growing body of air pollution mitigation methods that substantially improve outdoor air quality in different urban contexts. Generally, the improvement in outdoor air quality can be divided into two levels: (i) the utilization of mechanical factors for pollutant mitigation, including forced convection by ambient wind, natural convection by solar radiation, and traffic-induced convection due to traffic movement; (ii) the correlation between complex urban features and pollutant dispersion based on the sound design of the urban landscape and building geometries. This aspect focuses on improving the capacity to reduce air pollution by modifying the

urban morphology, including the urban density, heterogeneity, and degree of urban enclosure. Accordingly, it is crucial for urban planners to design the urban morphology appropriately and utilize mechanical factors to reduce the pollutant concentration.

Several state-of-the-art reviews have been published in related areas (mitigation of air pollution) in the past decade, focusing on the influence of trees [9,10], solid and porous barriers [11], urban planning strategies [12], and reactive pollutants [13]. Summaries of computational fluid dynamics (CFD) studies were also conducted [14–16]. Moreover, Peng et al. [17] summarized the main ventilation indices used to evaluate urban outdoor ventilation. Zhao et al. [18] conducted an in-depth review on theoretical, experimental, and numerical research on the isothermal and non-isothermal flow in street canyons. He et al. [19] analyzed urban surface structures for a systematic study of local ventilation performance. Going beyond the scope of existing reviews on this topic, three problems are worth noting. First, a complete summary of the fundamental mechanism of pollutant dispersion is lacking, including the influence of mean flow and turbulence. Second, most of the previous reviews only provided qualitative conclusions. Therefore, there is a need for a comprehensive survey of the quantitative reduction of pollutant concentrations for different influential factors. However, it is still difficult to ascertain which factors are most significant for determining air pollutant dispersion.

Therefore, the objectives of this review are to (i) describe the individual and combined effects of the mean flow and turbulence on pollutant dispersion, (ii) provide a detailed quantification of the reduction potential of each mechanical measure and urban morphology, and (iii) compare different mechanical measures and urban morphology to identify the critical urban factors for the development of practical urban optimizing strategies.

The review is conducted by searching for papers using the Web of Science, Science Direct, and Google scholar in addition to publications known to the authors. The literature search was performed in late 2020, and articles published until early 2020

were included. The keywords included “urban”, “pollutant dispersion”, “ventilation”, “outdoor”, and all the factors (all subtitles) mentioned in Sections 3 and 4. We combined all four keywords and each factor one by one for each search of the database to ensure the inclusion of studies dealing with pollutant dispersion mechanisms in urban areas. Only publications in English language journals were included.

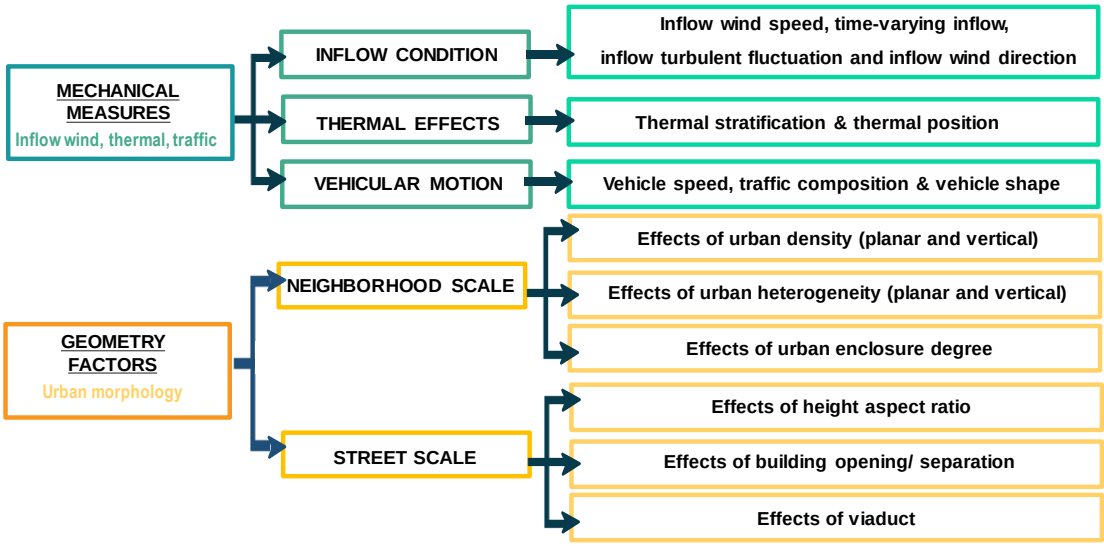

Fig. 1 Structure of the review

This paper provides a comprehensive and systematic review of the effectiveness of various pollutant dispersion mechanisms in the urban context (Fig. 1). Section 1 covers a brief overview of the two levels of influence on pollutant dispersion. Then, two basic pollutant dispersion processes (affected by mean flow and turbulence) are identified in Section 2. Sections 3-4 focus on the quantification of the dilution potential of different mechanical measures and urban morphology and the dominant dispersion processes. It is described how to utilize mechanical measures (effects of inflow conditions, thermal effects, and vehicular motion) and create a sound design of urban morphology (neighborhood scale: effects of urban density, heterogeneity, and enclosure degree; street scale: effects of height to aspect ratio, building opening/ separation, and viaduct). Finally, the conclusion is drawn in Section 5 to summarize the effectiveness of the two levels of influence on pollutant dispersion.

2. General characteristics of pollutant dispersion processes

A clarification of the basic processing governing pollution dispersion is required to understand the effect of mechanical factors and urban morphology on the dispersion and distribution of pollutants. The fluid flow around buildings is typically categorized as the mean flow and deviations from the mean (turbulence) [20–22]. There is a consensus among researchers that mean flow and turbulence play significant roles in the dispersion of pollutants [23,24].

We begin by describing the skimming flow in a two-dimensional (2D) infinite regular street canyon (which is the case in most studies in the literature, where the building height (H) / street width (W) = 1) (Fig. 2 (a)) to understand the influence of the mean flow and turbulence. In the presence of perpendicular ambient wind, a strong shear layer with a large velocity gradient is developed at the roof level of street canyons due to the flow separation at the leeward edge of the building [25]. Furthermore, clockwise recirculation occurs in the entire street canyon because of the entrained momentum from the top shear layer [26]. Once the pollutant is emitted from street-level vehicles, most pollutants will follow the primary recirculation (mean flow), causing a higher concentration at the leeward side of the street canyons [27] (Fig. 2 (b)). Then, the upward mass will transfer with the external flow at the roof level. However, a significant fraction of pollutants does not flow upwardly by vertical mean flux [28] because the vertical velocity is low [26]. Instead, the primary recirculation causes most pollutants to re-enter the street canyon by horizontal advection at the roof level [29]. In contrast, the pollutants escape from the street canyons mainly by the turbulent pollutant flux along the roof-top level [30]. Consequently, turbulent transport plays a dominant role in the wash-out process of pollutants through the top shear layer [29,31] (Fig. 2 (c)).

The three-dimensional (3D) street canyon flow is more complex than the 2D in-canyon flow [18]. As illustrated in Fig. 2(e) (a finitely long regular street canyon), the canyon vortex in the middle part of the street canyon (driven by the shear flow from

building roofs) interacts with the corner eddies at the ends of the street canyon (induced by the inflow from the sides of the upwind buildings) [32]. Different interactions of the canyon vortex and corner eddies caused by different street lengths will further influence the pollutant dispersion within the street canyon [33]. For instance, Michioka et al. [34] observed different pollutant fluxes at the roof level. As shown in Fig. 2(f), the turbulent pollutant fluxes for shorter canyons were larger than the mean pollutant fluxes, but these two fluxes were almost the same for longer canyons. The turbulent motion dominated pollutant removal for shorter canyons, and both the turbulence and the mean flow affected pollutant dilution for the longer canyons. Therefore, the contribution of the lateral shear layer in a 3D street canyon should also be considered [35,36], especially for a short distance [34], as illustrated in Fig. 2 (d).

In general, both mean flow and turbulence significantly affect the pollutant removal from the side or top of street canyons. Further, the mean flow and turbulence are affected by mechanical factors, such as the inflow velocity and turbulence intensity, the mean flow due to solar radiation, and traffic-induced turbulence sources at the ground level. Besides, a change in urban morphology will also significantly influence the mean and turbulent pollutant fluxes to different extents, which, in turn, determines the dispersion and distribution of pollutants in the urban context. All these influences will be discussed in Sections 3-4.

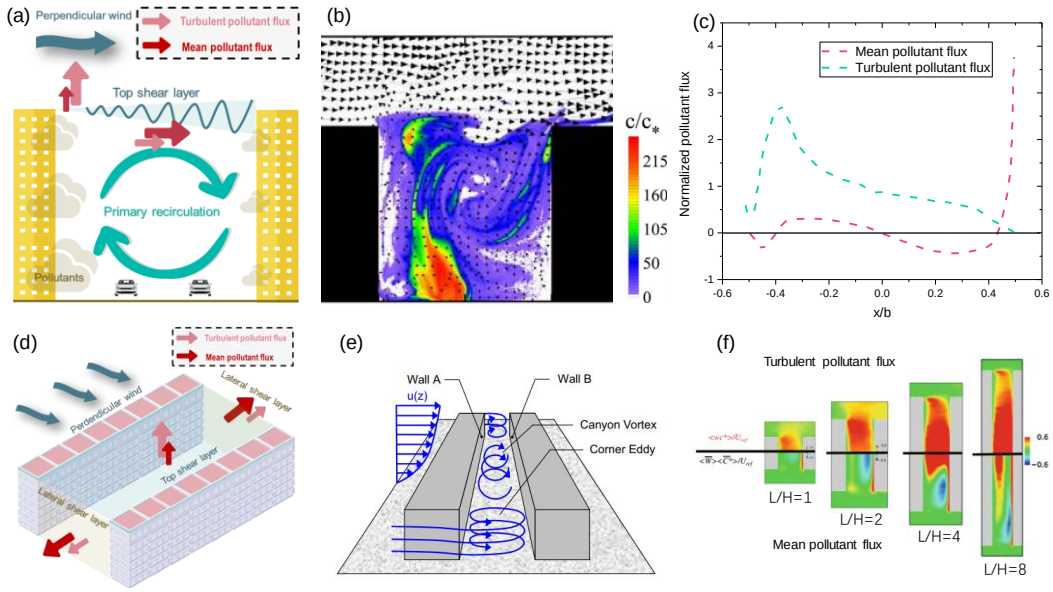

Fig. 2 (a) Side view of flow characteristic and pollutant dispersion processes in an infinitely long regular street canyon (H/W = 1), (b) instantaneous velocity (vectors) and concentration (colors) fields for the infinitely long regular street canyon[27], (c) profiles of mean pollutant flux and turbulent pollutant flux along the roof of street canyons (modified from [29]), (d) perspective view of pollutant dispersion processes in the top and lateral shear layers of a finite 3D street canyon, (e) flow field in and around a 3D street canyon [32], and (f) spatial variation of turbulent and mean pollutant fluxes at the roof level [34]. The pink and red arrows represent the turbulent and mean pollutant fluxes, respectively. The size of the arrow denotes the relative contribution of pollutant flux.

3. Effects of mechanical measures

3.1 Effects of inflow conditions

The inflow wind characteristics directly affect pollutant removal. With a growing focus on pollutant dispersion, an increasing number of research projects have explored the correlation between the inflow characteristics and the pollutant dispersion in a street canyon. The inflow wind components can be separated into three components as follows [25,37],

$$u = U + \tilde{u} + u' \tag{1}$$

where U is the spatially averaged mean wind speed, obtained by averaging the measurements over space and time; $\tilde{u}$ is the spatial fluctuation (low-frequency fluctuations), which is time-varying; u' is the turbulent fluctuation (high-frequency fluctuations) [38], which fluctuates randomly in time and space.

Therefore, studies on the inflow wind characteristics can be categorized into three groups: studies on the inflow wind speed, those on time-varying inflows, and those on inflow turbulent fluctuation. The influence of the inflow wind direction is also summarized.

3.1.1 Inflow wind speed

It is evident that the mean flow and turbulence level in canyons are both

influenced by the inflow wind speed. Usually, poor ventilation is directly related to low wind speed.

The mean flow patterns are sensitive to ambient wind speed [39]. DePaul and Sheih [40] conducted a field experiment in a street canyon with $H/W \approx 1.5$ and found that when the ambient wind exceeded a threshold value (nearly 2 m/s), the street canyon generated a stable rotating vortex driven by momentum transfer at the roof height. Above this critical value, the flow structure remained the same, regardless of the inflow wind speed, which also could be justified by the ‘‘Reynolds number (*Re*) independence’’ hypothesis[41]. $Re = U_{ref} H/v$, where U_{ref} is a reference wind velocity, and v is the kinematic viscosity of the fluid. As long as the *Re* exceeds a critical value, the flow structure around the buildings remains invariant with an increase in *Re*[42,43] (Fig. 3(a)). Kang et al. [44] reported that the critical *Re* for a street canyon with $H/W = 1$ is about 11,650. Moreover, it was found that the critical *Re* was between 57,000 and 87,000 in a deep street canyon ($H/W = 2$) [41]. Furthermore, Nakamura and Oke [45] conducted field observations of wind in the street canyons in Kyoto (Japan). The results suggested a relationship between the ambient wind speed and the in-canyon wind speed, i.e., $U_{canyon} = p_v \times U_{roof}$, where U_{canyon} denoted the in-canyon wind speed, and U_{roof} represented the ambient wind at the roof level. p_v was a diminution factor (<1) that depended on the street canyon H/W and the measurement levels (at a small H/W, p_v approached unity). In a regular street canyon ($H/W = 1$), the canyon and roof wind were 0.06 *H* and 1.2 *H*, $p_v \approx 2/3$. On the other hand, the in-canyon turbulence level was enhanced by increasing inflow wind speed. Nazridoust and Ahmadi [46] found that the turbulence intensity in the street canyon increased with an increase in ambient wind speed. When the inflow wind speed increased from 3 to 20 m/s, the turbulence intensity increased by nearly 16 times near the ground level and 7 times at the roof height (Fig. 3(b)). The reason is that at high wind speeds, the circulating flow is stronger, leading to higher turbulence fluctuation energy.

Since the mean flow and turbulence increase with increasing wind speed, the air

quality is expected to improve. Berkowicz et al. [47] confirmed the dependence of the normalized pollutant concentration on the ambient wind speed at the pedestrian level, i.e., $C^*= 0.18\times U_{roof}^{-0.46}$, where C^* denoted the normalized passive gaseous pollutant concentration (carbon monoxide （CO)) at the pedestrian level. Based on the ambient wind speed, the normalized concentration decreased by nearly 65.5% when the wind speed increased from 0.3 m/s to 3 m/s. Similarly, a 44.2% drop in the maximum passive gaseous pollutant concentration near the ground level (wind speed increased from 3 m/s to 20 m/s) [46] (Fig. 3(c)) and a 40.1% reduction in the maximum passive gaseous pollutant concentration (nitrogen dioxide (NO_2)) close to the leeward building surfaces (wind speed increased from 3 to 7 m/s) [48] were reported.

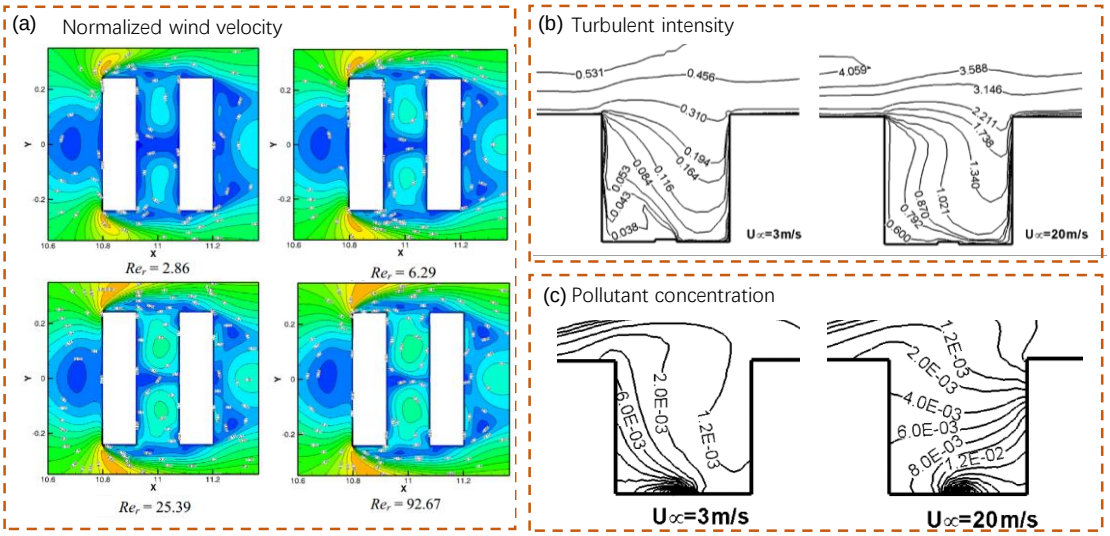

Fig. 3 (a) Changes in the normalized velocity contours at the pedestrian level for different Re_r[43]; (b) turbulence intensity (%) contours for different wind velocities [46] and (c) CO_2 mass fraction contours for different wind velocities [46]

Table 1 Overview of studies on the effect of inflow wind speed

Ref.	Focus	Urban configuration	Study approach	Remarks
[40]	a	S ($H/W \approx 1.5$)	FM	When the ambient wind exceeds a threshold value (nearly 2 m/s), the street canyon (H/W =1.5) generates a stable rotating vortex
[43]	a	S ($H/W \approx 1$)	CFD (V)	As long as the *Re* exceeds a critical value, the flow structure around the buildings remains invariant with an increase in *Re*
[45]	a	S ($H/W \approx 1$)	FM	There was a relationship between ambient wind speed and in-canyon wind speed, i.e., $U_{canyon}= p_v\times U_{roof}$
[46]	a, b, c	S ($H/W \approx 1$)	CFD (V)	The turbulence intensity in the street canyon increased with an increase in ambient wind speed; there was a 44.2% drop in the maximum pedestrian-level pollutant concentration (wind speed increased from 3 m/s to 20 m/s)

Focus: a = Mean flow, b = Turbulence, and c = Pollutant; **Urban configuration:** C = City, S= Street canyon, B = Building arrays, λ_F =

Frontal area density, *H/W* = Height aspect ratio (building height/ street width); **Study approach:** WT = Wind tunnel measurements, FM = Field measurements, CFD (V) = CFD with validation, and CFD (NO) = CFD without validation.

3.1.2 Time-varying inflow

Most previous studies assumed steady wind conditions and did not consider changes in the ambient wind velocity and direction [49]. However, field measurement data indicated that these two parameters always changed over time [38,50], referred to as time-varying inflows [51]. Unlike steady wind conditions, the time-varying inflows can significantly impact the flow structure downstream and the corresponding mass transport [52–54]. Li et al. [55] observed a downdraft in the peak period of gusty winds (a type of time-varying inflow) and an updraft in the valley period. Duan et al. [56] observed that incorporating time-periodic perturbations into the inflow boundary caused a small but statistically significant response to inflow perturbations in the turbulent flow in a street canyon. Similarly, Zhang et al. [57] revealed that the variations of the inflow conditions caused intermittent features in a street canyon, i.e., the expansion or compression of the air mass in the street canyon. Thus, the shear layer at the roof level was flapped with the time-varying inflows. Furthermore, Li et al. [58] pointed out that a gradual decrease in the inflow wind speed induced the upward movement of the main vortex, hence enlarging it, and vice versa (Fig. 4(a)). The time-varying inflows destroyed the strong shear layer at the rooftop level, thus significantly enhancing the vertical pollutant turbulence transport flux. Zhang et al. [57] observed that the pollutant flux under time-varying inflows was one order of magnitude higher than the steady inflow counterparts. Accordingly, Li et al. [58] reported that the time-varying inflow had a lower concentration than the steady inflow in the street canyon, as shown in Fig. 4(b). In an unsteady simulation, the average passive gaseous pollutant concentration in the entire street canyon was 36.7% lower than that under a steady flow half an hour after the pollutant release (Fig. 4(c)). The concentration at the pedestrian level decreased by nearly 42% after half an hour when the steady-state airflow field was the initial field in the time-varying inflow simulation. Therefore, Zhang et al. [59,60] concluded that the influence of time-varying inflows was significant and should

not be ignored.

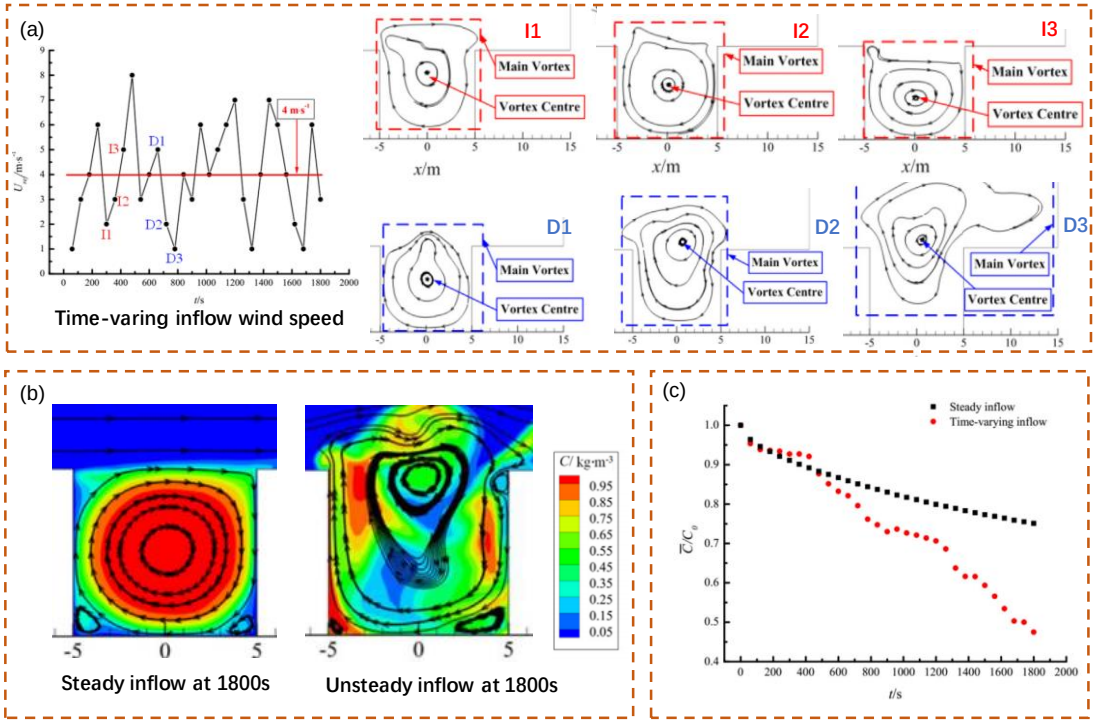

Fig. 4 (a) The movement of the main vortex corresponding to a change in the inflow [58]; (b) the change in the pollutant concentration and streamlines with time-varying inflows [58]; (c) the change in the normalized average pollutant concentration in the entire street canyon over time under steady inflow and time-varying inflow [58]

Table 2 Overview of studies on the effect of time-varying inflows

Ref.	Focus	Urban configuration	Study approach	Remarks
[56]	a	S ($H/W \approx 1$)	CFD (V)	Incorporating time-periodic perturbations into the inflow boundary caused a small but statistically significant response to inflow perturbations in the turbulent flow
[58]	a, c	S ($H/W \approx 1$)	CFD (V)	A gradual decrease in the inflow wind speed induced the upward movement of the main vortex, enlarging it, and vice versa; the average pollutant concentration in the entire street canyon was 36.7% lower than under steady flow half an hour after the pollutant release
[57]	a, c	S ($H/W \approx 1$)	CFD (V)	The pollutant flux under time-varying inflows was one order of magnitude higher than the steady inflow counterparts

Focus: a = Mean flow, b = Turbulence, and c = Pollutant; **Urban configuration:** C = City, S= Street canyon, B = Building arrays, λ_F = Frontal area density, H/W = Height aspect ratio (building height/ street width); **Study approach:** WT = Wind tunnel measurements, FM = Field measurements, CFD (V) = CFD with validation, and CFD (NO) = CFD without validation.

3.1.3 Inflow turbulent fluctuation

Inflow turbulent fluctuations can be interpreted as three-dimensional eddies with different length scales that constantly interact with each other [61]. It is well-known that the inflow turbulence properties significantly affect the flow field in urban areas

[62–64]. Numerous studies used CFD simulations of inflow turbulence generation to improve the prediction of the turbulence structure around buildings [63,65,66]. Moreover, the inflow turbulent fluctuation is also an essential parameter influencing the pollutant dispersion in urban areas. Kim and Baik [67] reported that the downward momentum transfer of the ambient flow into the street canyon was larger in an experiment with inflow turbulence than in the control experiment with no appreciable inflow turbulence. The authors found that part of the inflow turbulent eddies interacted with the horizontal flow at the roof-top level. The turbulent eddies intruded into the street canyon, enhancing the intensity of the canyon vortex. Further, Shi et al. [68] demonstrated that the pollutant concentration around buildings was increased if the inlet turbulence fluctuations were not included, as shown in Fig. 5(a).

Furthermore, Michioka et al. [34] investigated the influence of inflow turbulence intensity on the airflow and pollutant dispersion around buildings for different upstream urban geometries. The results suggested that different turbulence intensities of the external flow resulted in different pollutant removal efficiencies. The influence of inflow turbulence intensity on pollutant dispersion was primarily attributed to a change in the turbulent kinetic energy (TKE) rather than changes in the flow field. For instance, An et al. [69] reported that a significant change (50%) in the inflow turbulence intensity yielded less than a 15% change in the wind speed in the same urban area. As confirmed by Kim and Baik [70], even if there was a noticeable deviation (500%) in the inflow turbulence intensity, the average in-canyon wind speed and flow structure barely changed (Fig. 5(b)). Nonetheless, a higher level of inflow turbulence resulted in a smoother momentum distribution and a decrease in the peak of the wind speed. However, the in-canyon TKE was notably enhanced by the increasing inflow turbulence (Fig. 5(c)), directly affecting the pollutant removal potential. A ten-fold increase in the inflow turbulence led to an almost three-fold increase in the TKE in the street canyons, significantly reducing the pedestrian-level passive gaseous pollutant concentration by approximately 50% (Fig. 5(d)).

Besides, the incoming turbulent structure of the flow is another key parameter influencing the pollutant removal from urban areas. Michioka et al. [71] pointed out that the inflow turbulent motions, composed of coherent structures of low-momentum fluid and generated close to the roof level of the upstream, strongly affect the downstream pollutant removal. Michioka and Sato [72] studied three turbulent inflows with different coherent structures generated by three different upstream block configurations. The results showed that the size of the coherent structure was directly related to the amount of pollutant removal. The larger the size of the coherent structure, the greater the quantity of pollutants removed from the canyon was (Fig. 5(f)). A 44% change in the in-canyon spatially averaged passive gaseous pollutant concentration was observed with a change in the inflow turbulent structure.

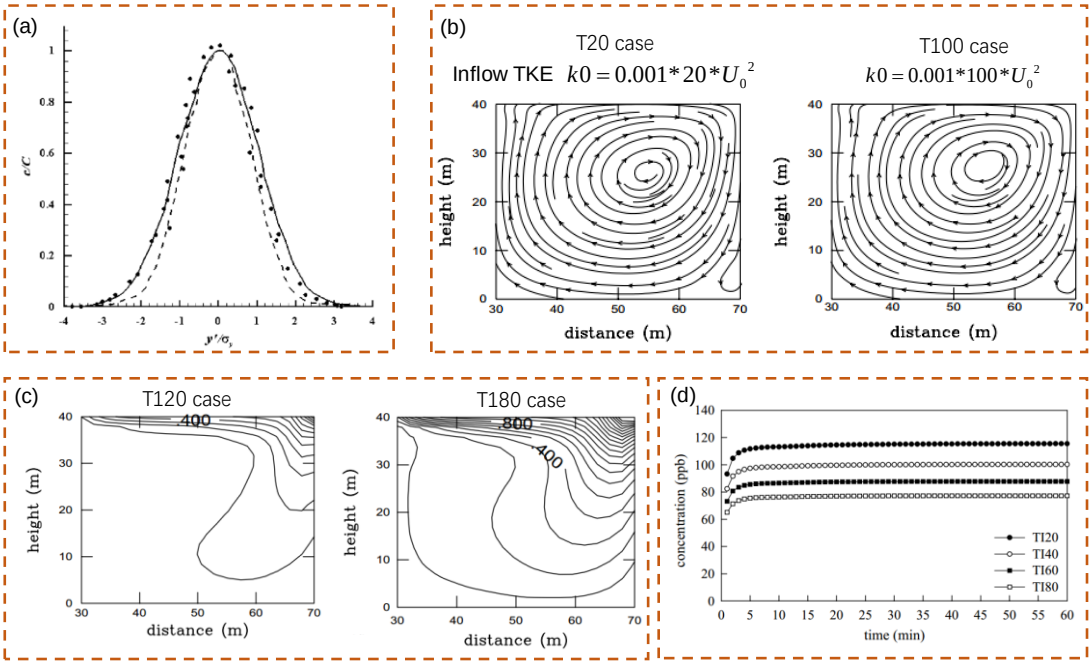

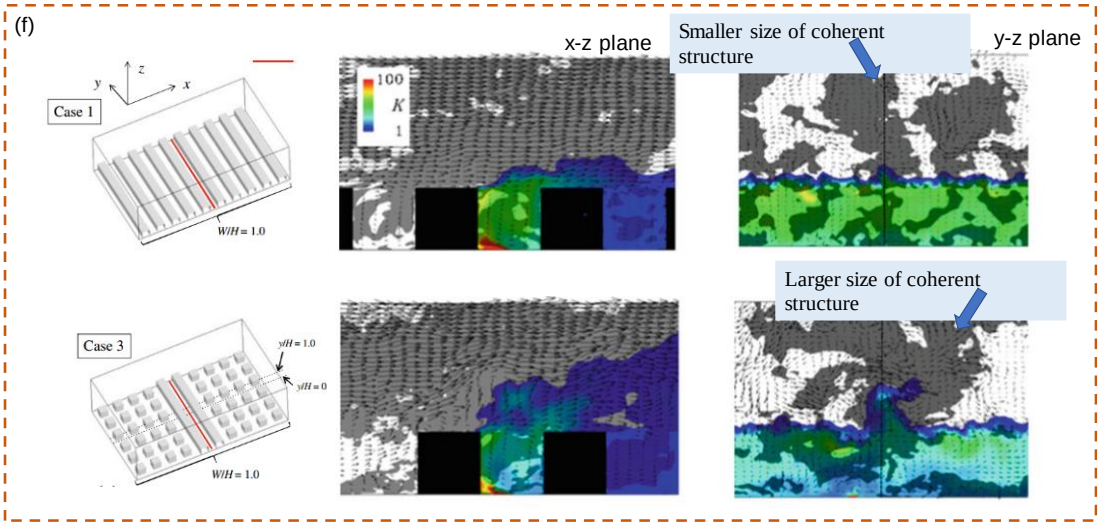

Fig. 5 (a) Concentration profile behind the fifth row; solid line: computation with inlet fluctuations; dashed line: computation without inlet fluctuations; dots: experimental measurements [68]; (b) streamline fields for different inflow turbulent intensities [70]; (c) turbulent kinetic energy fields for different inflow turbulent intensities [70]; (d) time series of pollutant concentration at z= 2 m of the street canyon center [70]; (f) instantaneous images of the low-momentum fluid (grey: u<0), instantaneous velocity vector, and concentration of tracer gas (colored contours) in the x–z and y–z planes [72].

Table 3 Overview of studies on the effect of inflow turbulent fluctuation

Ref.	Focus	Urban configuration	Study approach	Remarks
[68]	b, c	B	CFD (V)	A higher pollutant concentration was observed around the buildings if the inlet turbulent fluctuations were not included.
[69]	a, b, c	C	CFD (V)	A significant change (50%) in the inflow turbulence intensity yielded less than a 15% change in the wind speed in the same urban area.
[70]	a, c	S (H/W = 1)	CFD (V)	Even if there was a noticeable deviation (500%) in the inflow turbulence intensity, the average in-canyon wind speed and flow structure barely changed; a ten-fold increase in the inflow turbulence led to an almost three-fold increase in the TKE in the street canyons, significantly reducing the pedestrian-level concentration by approximately 50%.
[72]	a, b, c	S (H/W =1)	CFD (V)	The size of the coherent structure was directly related to the amount of pollutant removal; a larger size of the coherent structure caused a greater quantity of pollutant removed from the canyon

Focus: a = Mean flow, b = Turbulence, and c = Pollutant; **Urban configuration:** C = City, S= Street canyon, B = Building arrays, λ_F = Frontal area density, H/W = Height aspect ratio (building height/ street width); **Study approach:** WT = Wind tunnel measurements, FM = Field measurements, CFD (V) = CFD with validation, and CFD (NO) = CFD without validation.

3.1.4 Inflow wind direction

The inflow wind direction is another critical parameter of the flow structure (the number and shape of vortices) in the canyons, thereby determining the in-canyon

pollutant concentration [13]. Wise et al. [73] reported that a small change in the wind direction resulted in a substantial change in the flow characteristics of urban areas. For instance, the authors found that a 15° change in the wind direction led to a maximum 7% change in the space-averaged wind velocity at 20 m elevation.

Herein, the incident wind angle θ is defined as the angle between the wind direction and the street axis. Thus, $\theta = 0$ ° denotes that the wind direction is parallel to the direction of the street axis, whereas $\theta = 90$ ° represents the perpendicular direction. It is noteworthy that the effects of the wind direction on the flow characteristics differ for different types of urban geometries, especially for the street length (a long street canyon and a short street canyon). The dependencies of the pollutant concentration on the external wind direction and street length are somewhat contradictory [74]. Thus, the influence of the wind direction will be discussed for long street canyons (street length (L) /building height (H) > 7) and short street canyons (L/H < 3), based on the classification of Vardoulakis et al. [75].

Nakamura and Oke [45] concluded that a long street canyon generated a stable vortex for perpendicular wind, whereas a channeling wind was observed for parallel wind. However, oblique wind-induced a spiral vortex along the length of the canyon (a "cork-screw" action). Accordingly, the in-canyon velocity was affected by different flow patterns. Buller [76] obtained measurements of the inflow wind direction in residential areas in towns in England. The results showed that the general relation between the ambient and in-canyon wind speed was almost linear (i.e., $U_{canyon}=p\times U_{roof}$, where the value of p is related to the wind direction). The value of p increased gradually as the wind direction changed from perpendicular to parallel; these results were confirmed by Nakamura and Oke [45]. The value of p was between 0.37 and 0.75 [45], as shown in Fig. 6(a). Thus, it was deduced that the lowest in-canyon wind speed occurred during perpendicular wind conditions. Schatzmann and Leitl [77] and Kastner-Klein and Plate [78] revealed that perpendicular wind yielded the maximum pollutant concentration, whereas parallel wind resulted in the minimum concentration.

In their research, a nearly 67% reduction in the passive gaseous pollutant concentration (SF_6) at the pedestrian level was observed when the wind direction changed from perpendicular wind to parallel wind (Fig. 6 (b)). In light of this situation, most previous studies on pollutant dispersion focused on the worst pollution scenarios under perpendicular wind conditions [79]. Interestingly, Blackman et al. [80] argued that when the street length was sufficiently long (i.e., L/W= 12, where L is the length of the street canyon), the pedestrian-level pollutant concentrations of parallel wind and perpendicular wind conditions were comparable.

Regarding studies on short street canyons, Kim and Baik [81] investigated the effects of the wind direction ($45° < \theta < 90°$) on the flow and concentration of passive gaseous pollutants in a 4×4 matrix of buildings with a frontal area density (FAD) of λ_F = 0.25 (λ_F is the ratio of the frontal area to the total surface area of the building). Interestingly, worse air quality was found when $\theta = 45°$, which is different from the cases of a long street (Fig. 6 (d)). When θ increased from 45° to 90°, the total resident time of pollutants (the ratio of the total amount of pollutants remaining around the building arrays) decreased by about 34.3%. Similarly, Lin et al. [82] reported that better ventilation efficiency was observed for $\theta = 90°$ than for oblique wind directions for a 7×7 matrix of buildings (Fig. 6 (c)). The reason is that oblique wind has considerably more flow resistance. Also, Ramponi et al. [83] stated that the most favorable dispersion conditions were attributed to perpendicular wind due to a stronger channeling effect. As θ decreased from 45° to 0°, the maximum passive gaseous pollutant retention time decreased from 1.8 to 0.8.

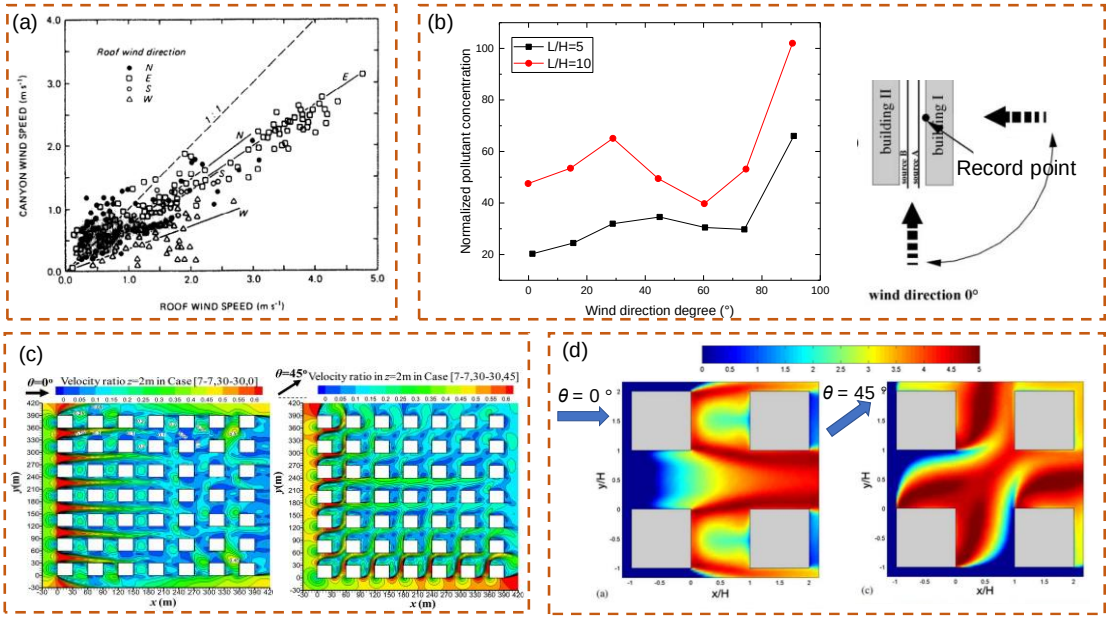

Fig. 6 (a) The relationship between the wind speed 3.6 m above the roof and 1.0 m above the center of the canyon floor for different wind directions [45]; (b) the influence of the wind direction on the pollutant concentration at the level z/H= 0.083 in long street canyons [78]; (c) the influence of the wind direction on the velocity ratio at z = 2 m for building arrays [82]; (d) the influence of the wind direction on the normalized pollutant concentration at z/H=0.17 for building arrays [81]

Table 4 Overview of studies on the effect of inflow wind direction

Ref.	Focus	Urban configuration	Study approach	Remarks
[73]	a	C	CFD (V)	In urban areas, a 15° change in the wind direction leads to a maximum 7% change in the space-averaged wind velocity.
[45]	a	S ($H/W \approx 1$)	FM	In a long canyon, perpendicular/parallel/oblique wind causes a stable vortex/ channeling wind/spiral vortex.
[76]	a	S	FM	In a long canyon, $U_{ped}=p\times U_{roof}$ (p increases as the wind direction changes from the perpendicular direction to the parallel one)
[78]	a, c	S ($H/W = 1$)	WT	In a long canyon, nearly 67% reduction in the concentration is observed when the wind direction changes from perpendicular wind to parallel wind.
[82]	a	B ($\lambda_F = 0.25$)	CFD (V)	For a building array with short canyons, better ventilation efficiency is observed for $\theta = 90°$ than for oblique wind directions.
[81]	a, c	B ($\lambda_F = 0.25$)	CFD (V)	For a building array with short canyons, the total resident time of the pollutant decreases by about 34.3% as θ increases from 45° (oblique) to 90° (perpendicular).

Focus: a = Mean flow, b = Turbulence, and c = Pollutant; **Urban configuration:** C = City, S= Street canyon, B = Building arrays, λ_F = Frontal area density, H/W = Height aspect ratio (building height/ street width); **Study approach:** WT = Wind tunnel measurements, FM = Field measurements, CFD (V) = CFD with validation, and CFD (NO) = CFD without validation.

3.2 Thermal effects

When the wind is relatively weak in an urban area, thermal effects have a profound impact on the flow structure [84]. As reported by Liu et al. [85], the airflow

in canyons could be entirely driven by buoyant force when the external flow was calm. Accordingly, the thermal-induced flow should be considered as a fundamental driving force for pollutant dispersion in street canyons [86]. Most recently, studies on thermal effects have been performed. The primary concerns regarding the thermal effects can be categorized into those related to thermal stratification (neutral, unstable, and stable) and those concerning the thermal position (different surface heating configurations). In addition, the influence of wind is considered in the discussion of the thermal effects in this section.

3.2.1 Thermal stratification

Thermal stratification has non-negligible effects on the dispersion process in street canyons [87]. Usually, unstable stratification occurs in the daytime because substantial solar radiation received by building facades or road pavement results in large temperature differences between urban surfaces and the air (exceeding 10 ℃ [88]). Unstable stratification is also observed at night due to the urban heat island phenomenon [45]. Apart from this situation, the nocturnal flow remains thermally stable [89]. The bulk Richardson number Ri (or R_b) was used to characterize thermal stratification quantitatively [90]. $Ri = gH\,(T_H\text{-}T_0)/\{(T\text{+}273)\,(U_H)^2\}$, where T is the mean air temperature (°C), T_H is the temperature at the top of the street canyon (°C), and T_0 is the ground temperature (°C). A negative Ri indicates unstable stratification (the urban surface is heated) [91], and a positive Ri indicates stable stratification (the surface is cooled) [92]. In general, thermal stratification affects pollutant dispersion by altering the mean flows and turbulence levels [93].

For mean flows, the primary circulation (canyon vortex) in the street canyon is enhanced in unstable conditions, whereas the in-canyon flow tends to be significantly slowed down in stable conditions. For example, Uehara et al. [90] conducted wind tunnel experiments to investigate the effects of different thermal stratifications ($-0.21<Ri<0.79$) on the flow in the canyons. The reverse flow speed during unstable stratification at the bottom of the street canyon increased by almost 60% compared to

the neutral case. Contrarily, this flow speed decreased to zero for a stable stratification (Fig. 7(a)). Also, a similar phenomenon was observed by Li et al. [89,94] and Cheng et al. [95]. Further, Cheng et al. [95] and Shen et al. [96] observed a stagnant region near the ground (z/h<0.15/0.1) under stable stratification, which complicated the dispersion of traffic emissions to the upper layers (Fig. 7(c)). As stated by Li et al. [89], this stagnation region resulted in the accumulation of approximately half of the pollutant amount in the lower part of the canyon. Cheng et al. [95] reported that a decrease in Ri from 0.35 to -0.11 reduced passive gaseous pollutant retention time by nearly 90% at the pedestrian level (Fig. 7(c) and (d)). Moreover, Li et al. [97] investigated the thermal effects in different street canyons with aspect ratios of 1, 2, and 0.5 for the same ground-heating intensity. Significant changes were observed in the flow patterns in the street canyon with H/W = 2 and 0.5, whereas the street canyon with the aspect ratio of 1 did not show any significant change in the flow field. Only the flow regime of the canyon with H/W = 0.5 was changed by ground heating (from wake interference flow to skimming flow).

Regarding the distribution of in-canyon turbulence, Li et al. [97,98] found that unstable stratification significantly enhanced the turbulence level inside the canyons. The possible reason is that turbulent transport was higher due to stronger primary recirculation when Ri< 0 compared to the neutral condition [99]. On the other hand, Park et al. [100] pointed out that the turbulence at the roof level was the result of changes in the streamwise horizontal velocity in the neutral condition. However, the buoyant flow increased the ratio of vertical velocity variance to turbulence at the roof level in an unstable condition. Rises in turbulence were observed at the rooftop, further enhancing the in-canyon turbulence level. Jiang et al. [101] showed that the TKE in urban canopies increased gradually with a decline in Ri, which was confirmed by Cheng et al. [99] (Fig. 7(b)). Also, Cheng et al. [99] reported that a slower canyon vortex in stable conditions resulted in a reduction in turbulent transport in the canyons. Thus, the turbulence level was reduced under stable stratification conditions, especially in the

lower part of the canyons. Furthermore, Jiang et al. [101] observed an inversely proportional relationship between the turbulence level and the mean pollutant concentration in the canyons, indicating that unstable stratification improved the turbulent pollutant flux, but stable stratification reduced it. Likewise, Li et al. [30] found that there was a substantial difference in the vertical turbulent transport for different levels of thermal stratification. Unstable stratification improved the vertical turbulent transport along the leeward surface, whereas neutral and stable stratification suppressed this transport process, especially during stable stratification. Thus, the efficiency of turbulent transport decreases with increasing *Ri*.

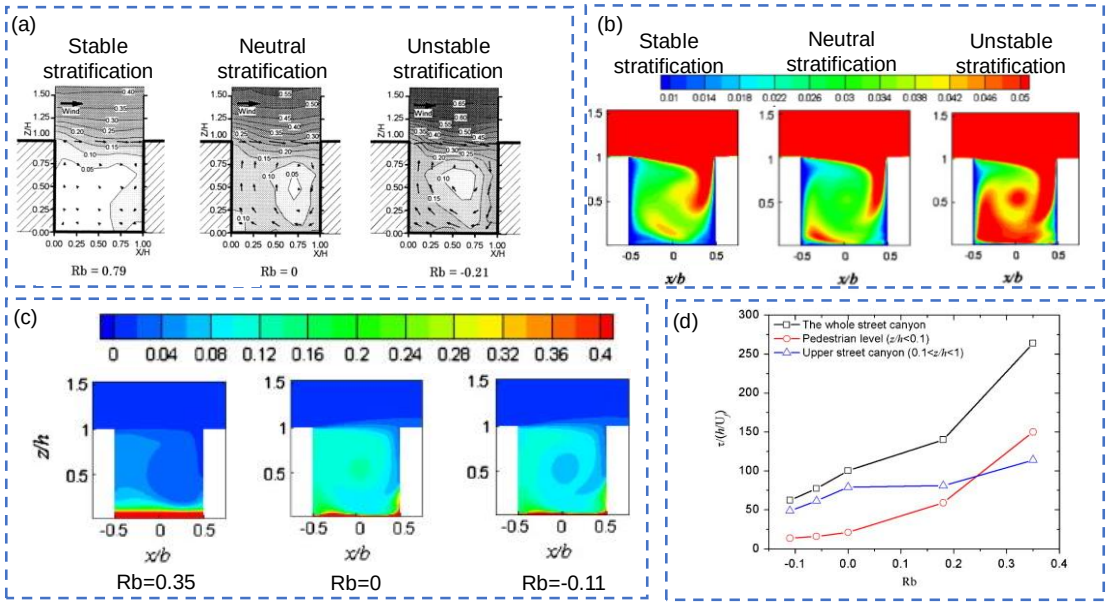

Fig. 7 (a) Normalized wind velocity in a street canyon (H/W =1) for different thermal stratifications [90]; (b) contours of $\langle u''u'' \rangle^{0.5} / U_{ref}$ in a street canyon (H/W =1) for different thermal stratifications [99]; (c) contours of normalized pollutant concentration for different thermal stratifications [99]; and (d) pollutant retention time (τ) versus R_b[99].

Table 5 Overview of studies on the effect of thermal stratification

Ref.	Focus	Urban configuration	Study approach	Remarks
[90]	a, b	S (H/W =1)	WT	The ground-level velocity of unstable stratification (Ri<0) was nearly 40%-60% higher than that when Ri= 0 (neutral), but it was weak (about zero) for stable stratification (Ri>0).
[96]	a, c	B (λ_F = 0.25)	CFD (V)	There was a stagnant region near the ground (z/h<0.15/0.1) under stable stratification, which complicated the dispersion of traffic emissions to the upper layers.
[98]	a, b, c	S (H/W =1)	CFD (V)	Unstable stratification significantly enhanced the turbulence level inside the canyons.
[95]	a, b, c	S (H/W =1)	CFD (V)	A decrease in Ri from 0.35 to -0.11 reduced pollutant retention time by nearly 90% at the pedestrian level

Focus: a = Mean flow, b = Turbulence, and c = Pollutant; **Urban configuration:** C = City, S= Street canyon, B = Building arrays, λ_F = Frontal area density, H/W = Height aspect ratio (building height/ street width); **Study approach:** WT = Wind tunnel measurements, FM = Field measurements, CFD (V) = CFD with validation, and CFD (NO) = CFD without validation.

3.2.2 Thermal position

During the daytime, different urban surfaces are heated by solar radiation at different angles (zenith angle) [102,103], as seen in Fig. 8(a). Solar radiation received by different surfaces heats the nearby air, increasing the buoyancy near the surfaces [104]. The thermal position has a profound impact on airflow and pollutant dispersion [105]. Usually, four heating scenarios are adopted to represent different times, i.e., ground heating (noon), leeward heating (morning or afternoon), windward heating (morning or afternoon), and all-wall heating (nighttime) [106]. As reported by Cai [107,108], different thermally induced flows combined with mechanically induced flows affect the flow field and the distribution of pollutants in two different ways: 1) *assisting*, the buoyancy takes effect in the same direction as the primary recirculation, 2) *opposing*, the buoyancy has the opposite direction as the mechanically induced flow.

Studies were conducted on mean flows caused by different thermal positions. For example, Allegrini et al. [109] conducted a wind tunnel experiment to study the flow characteristics in an infinitely long street canyon (H/W =1) with different heated surfaces. As shown in Fig. 8(b), the results showed that the ground, leeward, and all-surface heating scenarios hardly altered the flow structure compared with the neutral case; thus, there only existed primary recirculation in the center of the canyons. However, the in-canyon wind velocity was improved by the three heating scenarios, and the effect was especially pronounced for the ground heating scenario. In contrast, a secondary counter-rotation vortex appeared on the windward side in the windward

heating scenario. These results were confirmed by Kim and Baik [110] and Park and Baik [100]. In addition, Kim and Baik [110] pointed out that the upper-layer vortex was driven by mechanically induced flow, whereas the lower-layer vortex was thermally induced by the buoyant force when the windward surface was heated. In this heating scenario, the buoyancy had the opposite direction as the mechanically induced flow on the windward side, reducing the windward wind velocity to nearly zero. Therefore, the passive gaseous pollutant residence time in the canyon was nearly three times higher than those in the other heating scenarios. Similarly, Hang et al. [106] found that the maximum passive gaseous pollutant concentration (CO) near ground level could be reduced by nearly 80% when the heating scenario changed from windward heating to neutral. However, Lin et al. [111] obtained different results when the ambient wind speed changed. At a low wind speed, an updraft flow rather than the primary vortex existed in all heating scenarios. However, at high wind speed, a primary vortex formed only when the ground was heated, and the updraft flow dominated the canyons in the other heating scenarios. A possible explanation for this difference is the difference in thermal intensities and canyon geometries [112]. Regarding turbulence levels caused by different thermal positions, Park and Baik [100] found that ground heating resulted in a higher in-canyon turbulence level since the canyon flow was more intermittent and fluctuating compared with the windward heating scenario. Furthermore, Allegrini et al. [109] found that the ground, windward, and all-surface heating scenarios resulted in high levels of turbulence due to the combination of thermal-induced flow and mechanically induced flow (Fig. 8(c)). The level of turbulence was highest in the all-surface heating scenario.

It is noteworthy that the reviewed studies were mainly based on the assumption of uniform wall temperature. In effect, as stated by Li et al. [113,114], solar heating causes a non-uniform wall temperature, as shown in Fig. 8 (e). Thus, the influence of the thermal position on the flow structure should be different when solar heating is considered [115–120]. For instance, Nazarian et al. [121] observed a main vortex in the

canyons in all heating scenarios, and the ground and windward heating scenarios had the lowest and highest reverse velocity near the ground level, respectively. Furthermore, Nazarian et al. [119,120] reported that the volume-averaged pollutant concentration under an assumption of 3D non-uniform heating in the canyons first decreased until 1300 local time (*LT*) and then increased, resulting in a parabolic diurnal variation. Besides, ground heating still resulted in the lowest pollutant concentration, and the concentration in the windward heating scenario was still higher than that of the leeward heating scenario. From 0800 to 1300 *LT* or 1800 to 1300 *LT*, the passive gaseous pollutant concentration decreased by nearly 40% (Fig. 8 (f)).

Table 6 Overview of studies on the effect of thermal position

Ref.	Focus	Urban configuration	Study approach	Remarks
[109]	a, b	S (H/W = 1)	WT	Only primary recirculation occurs in the center of the canyons during ground, leeward, and all-surface heating, whereas a secondary counter-rotation vortex occurs in windward heating; ground heating causes the strongest ground-level wind velocity; ground, windward, and all-surface heating scenarios yield high levels of turbulence.
[106]	a, c	S (H/W = 0.5 to 3)	CFD (V)	The maximum pedestrian-level pollutant concentration could be reduced by nearly 80% when the heating scenario changed from windward heating to neutral
[113]	a, c	B (λ_F = 0.125 to 1.25)	CFD (V)	Realistic solar heating causes a non-uniform wall temperature
[116, 117]	a, b, c	B (λ_F = 0.25)	CFD (V)	Volume-averaged pollutant concentration under an assumption of 3D non-uniform heating in the canyons first decreased until 1300 local time and then increased, resulting in a parabolic diurnal variation

Focus: a = Mean flow, b = Turbulence, and c = Pollutant; **Urban configuration:** C = City, S= Street canyon, B = Building arrays, λ_F = Frontal area density, H/W = Height aspect ratio (building height/ street width); **Study approach:** WT = Wind tunnel measurements, FM = Field measurements, CFD (V) = CFD with validation, and CFD (NO) = CFD without validation.

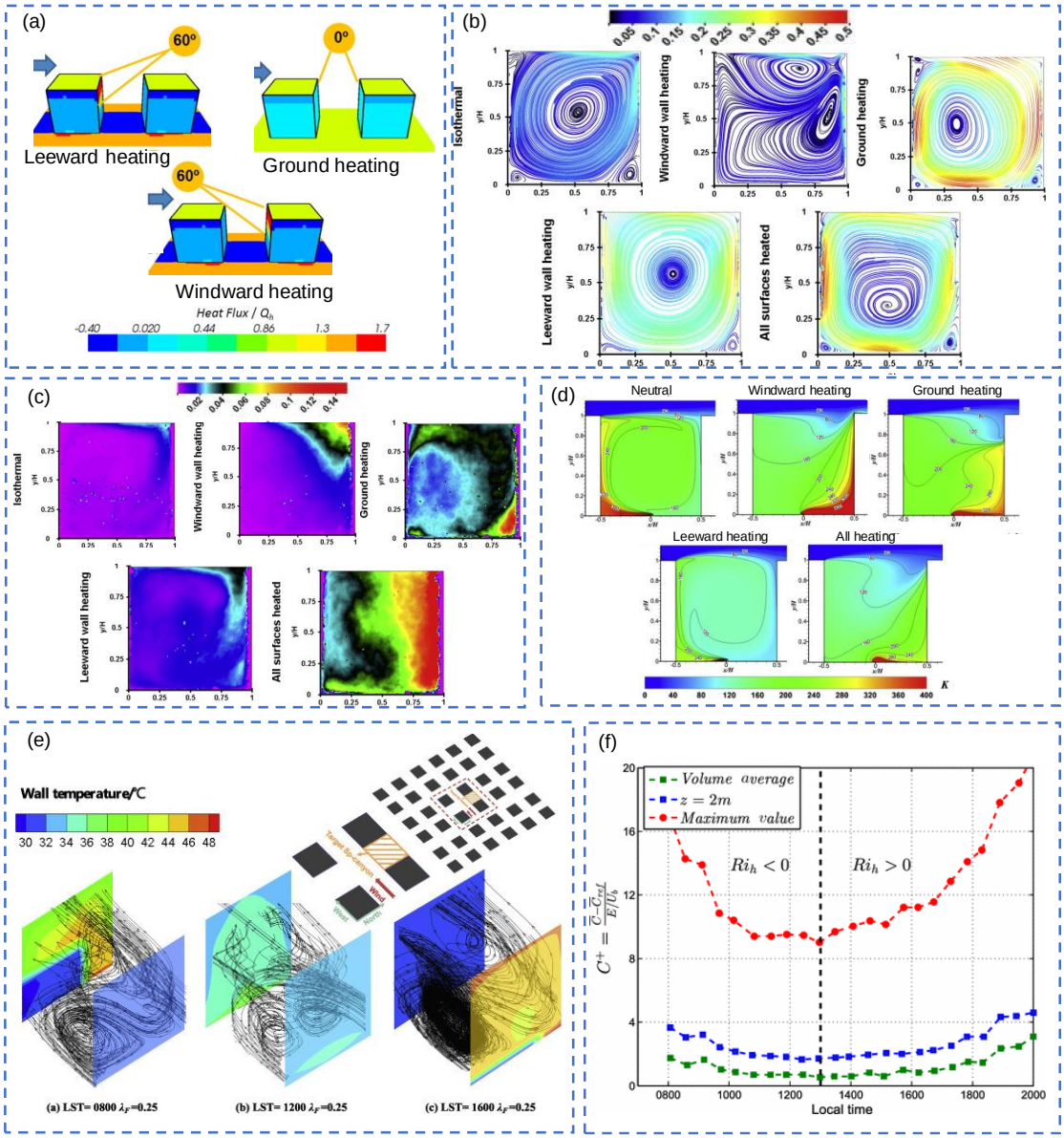

Fig. 8 (a) Surface sensible heat flux distribution normalized by the total heat flux above the canopy corresponding to different thermal positions [103]; (b) contour plots of the normalized velocities for various configurations of heated surfaces [109]; (c) contour plots of the normalized TKEs for various configurations of heated surfaces [109]; (d) contour plots of the normalized concentration for various configurations of heated surfaces [106]; (e) predicted wall temperature and 3D streamlines at different solar times [113]; and (f) changes in the normalized concentration over time [119,120]

3.3 Effects of vehicular motion

The findings of previous studies show that vehicular motion contributes significantly to pollutant dispersion in urban areas, especially at low wind speeds

[122,123]. The pollutant concentration in a street canyon may be underestimated when vehicular traffic is not considered [124,125]. The reason is the strong airflow at the bottom of street canyons due to ambient wind and the interactions with the movement of vehicles [126]. Jicha et al. [127] reported that if the vehicular motion was not considered in studies on pollutant dispersion, one of the most important factors influencing the mixing processes of pollutants in the canopy layer was ignored. Thus, the study of airflow and turbulence induced by vehicular motion is crucial to understand the dispersion process of pollutants in urban areas [128]. To date, some studies conducted field measurements, wind tunnel experiments, and numerical simulations to provide detailed descriptions of significant flow mechanisms affected by vehicle dynamics, i.e., traffic-produced turbulence (TPT) and traffic-produced flow (TPF).

Enhanced turbulence (TPT) near the target road was observed in most studies. For instance, Shi et al. [129] reported that moving vehicles generated a continuous turbulence source at the bottom of the canyons, which is in line with other studies [130–133]. Further, Qin and Kot [122] found that TPT significantly influenced the distribution of turbulence up to a height of approximately 7 m. Even at 30 m downstream of the traffic flow, Sedefians et al. [134] observed that the contribution of TPT to the total turbulence was as high as 50%. Accordingly, the reduction in the pollutant concentration in the traffic region is attributed to higher TKE near the ground level [129]. Besides, both Kondo and Tomizuka [133] and Woodward et al. [135] reported that the maximum pollutant concentration was reduced, and the peak was smoothed out in the direction of traffic flow due to TPT.

In addition to causing an increase in TKE by TPT, the vehicular motion also enhances the advection by entraining masses of air in the moving direction [127,136]. Therefore, TPF is also a crucial factor affecting pollutant dispersion in the close vicinity of moving traffic. For instance, Kondo and Tomizuka [133] observed a substantial difference in the flow fields of cases with and without TPF in two-way traffic. When the traffic movement was included in the model, two prevailing airflows with opposite

directions were observed in the streets. Furthermore, the authors compared the contribution of TPT and TPF to the reduction in pollutant concentration. TPF led to a reduction in pollutant concentration of as much as 40% at a monitoring post. In contrast, the influence of TPT on pollutant dispersion was greater than that of TPF (concentration declined by almost 50%).

In effect, the influence of vehicular motion (both TPT and TPF) is strongly correlated to the vehicle speed, vehicle shape, traffic volume, and traffic composition. These factors will be discussed below.

3.3.1 Vehicle speed

Wang et al. [137] studied vehicle-induced turbulence using dynamic mesh technology. The moving vehicles were assumed to have the same geometric shape (4 m length, 1.6 m width, and 1.4 m height), representing a small passenger car in China. The results indicated that the maximum TKE increased from 0.15 to 0.85 m^2/s^2 near roadways when the vehicle speed increased from 18 to 54 km/h (Fig. 9 (a)). The TKE rose to 10 m^2/s^2, with an increase in vehicle speed to 140 km/h [138]. Kastner-Klein et al. [131] found that the passive gaseous pollutant concentration at a reference point at ground level was reduced by almost 42% with a three-fold increase in vehicle (car) speed (Fig. 9 (b)). Similarly, Li et al. [123] found that in regions behind the moving vehicles (passenger car), the passive gaseous pollutant concentration significantly decreased because of the increasing vehicle speed.

3.3.2 Traffic composition

The traffic composition changes the distribution of TPF and TPT [139], and the effect is more pronounced for TPF. Pospisil and Jicha [139] assessed the pollutant dispersion of one-way and two-way traffic (car). The results showed that the passive gaseous pollutant concentration of two-way traffic at the pedestrian level was almost 44% higher than that of one-way traffic. These results were confirmed by Kastner-Klein et al. [131] (Fig. 9 (d)). In contrast, He and Dhaniyala [138] found that the TKE of two-way traffic (passenger cars) was approximately two times higher than that of one-way

traffic (Fig. 9 (c)). A possible explanation was proposed by Kastner-Klein et al. [131], who found that one-way traffic caused a more significant flow in the street direction, with mean velocities of 0.15 U_{ref} (U_{ref} is the ambient wind speed). Thus, TPF caused by one-way traffic results in the transport of pollutants in the direction of the canyon, leading to a reduction in the pollutant concentration.

3.3.3 Vehicle shape

Cai et al. [140] investigated the relationship between TPT and vehicle shape. The results indicated that a truck produced more TKE than a car or SUV in the canyons (Fig. 9 (f)). Furthermore, a high turbulence level can contribute to the mixing of pollutants and creates a more uniform pollutant distribution at the pedestrian level.

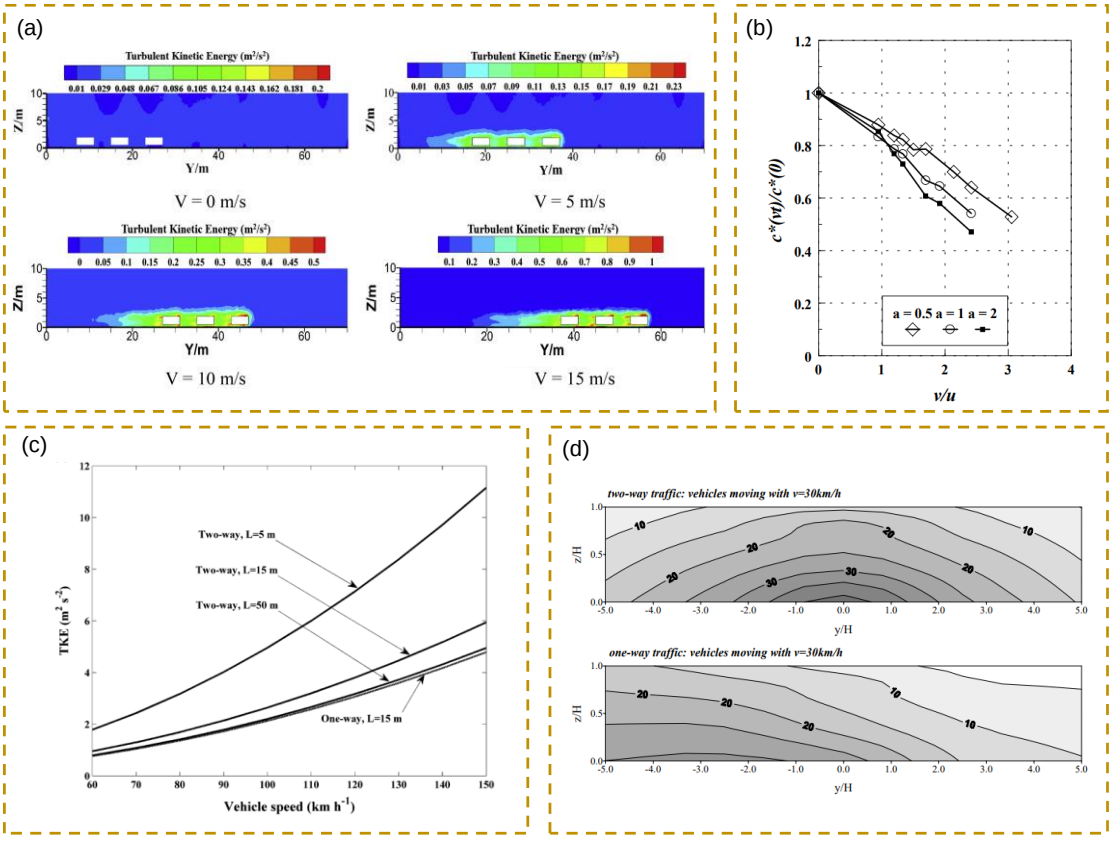

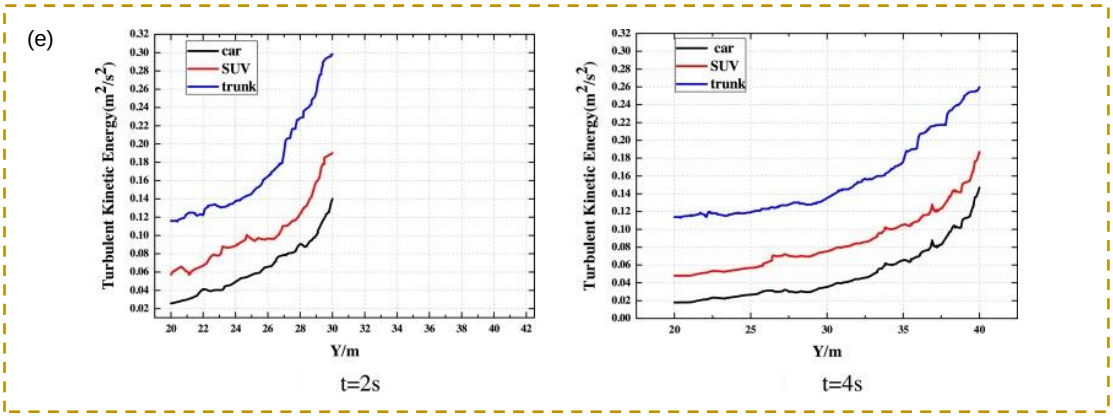

Fig. 9 (a) TKE contours across the centerline of vehicles at different velocities [137]; (b) normalized concentration at a reference point (leeward canyon wall, ground level) as a function of the velocity ratio v (vehicle moving speed) /u(reference wind speed); the traffic density is expressed by the scaling factor a [131]; (c) TKE profiles at different vehicle speeds and different distances to the opposing roadway (L=5, 15, 50 m) [138]; (d) concentration patterns at the leeward canyon wall for different traffic conditions [131]; (f) TKE distribution at the center height of the vehicle for different vehicle shapes [140].

Table 7 Overview of studies on the effect of vehicular motion

Ref.	Focus	Urban configuration	Study approach	Remarks
[129]	a, b, c	S (H/W = 1)	CFD (V)	Moving vehicles generate a continuous turbulence source at the bottom of the canyons
[127]	a, b, c	S ($H/W \approx 0.8$)	CFD (NO)	Vehicular motion enhances the advection by entraining masses of air in the moving direction
[133]	a, b, c	C	CFD (V)	Maximum pollutant concentration is reduced and the peak is smoothed out in the direction of traffic flow due to TPT
[137]	a, b, c	S (H/W = 1)	CFD (V)	The maximum TKE increased from 0.15 to 0.85 m^2/s^2 near roadways when the vehicle speed increased from 18 to 54 km/h
[131]	a, b, c	S (H/W = 1)	CFD (V)	Pollutant concentration at a reference point at ground level was reduced by almost 42% with a three-fold increase in vehicle speed
[139]	a, b, c	S (H/W = 0.8)	CFD (NO)	The traffic composition changes the distribution of TPF and TPT, and the effect is more pronounced for TPF; the passive gaseous pollutant concentration of two-way traffic at the pedestrian level was almost 44% higher than that of one-way traffic
[140]	a, b, c	S (H/W = 1)	CFD (V)	A truck produced more TKE than a car or SUV in the canyons

Focus: a = Mean flow, b = Turbulence, and c = Pollutant; **Urban configuration:** C = City, S= Street canyon, B = Building arrays, λ_F = Frontal area density, H/W = Height aspect ratio (building height/ street width); **Study approach:** WT = Wind tunnel measurements, FM = Field measurements, CFD (V) = CFD with validation, and CFD (NO) = CFD without validation.

3.4 Interactions between the three mechanical factors

3.4.1 Interactions between inflow conditions and thermal effects

Usually, the Richardson number, Ri ($\approx Gr/Re^2$) is used to compare the mechanical

driving force with the buoyant driving force, where *Gr* is the Grashof number, which is proportional to the buoyancy force, and *Re* is the Reynolds number, which is proportional to the mechanical force [112]. In most studies, *Ri* is 1. For instance, Offerle et al. [141] and Louka et al. [88] used field measurement and reported that the *Ri* was -0.59 and -4.42, respectively. Likewise, $|Ri|$ ranged from 0 to 10 in most studies that used wind tunnel experiments [90,109,111] or CFD simulations [99,115,142,143]. The absolute value of *Ri* represented the stable and unstable stratification simultaneously. Therefore, we can expect that the mechanical driving force and buoyant driving force both influence pollutant dispersion in most studies. Xie et al. [144] investigated the air exchange rate (AER) for various *Re* values and heating intensities of the ground in a street canyon. It was found that at the same *Re* value, an increase in the heating intensity increased the AER by 2-4 times. In contrast, at the same heating intensity, a decrease in *Re* increased the AER from 67% to 201%. Essentially, altering either the inflow wind speed or thermal effect resulted in pollutant dispersion. Furthermore, similar results were observed for different wind directions [117] and even different thermal positions [109,111,143].

3.4.2 Interactions between inflow conditions and vehicular motion

As mentioned in Section 3.3, vehicular motion causes more significant changes in the turbulence level than the mean wind velocity. Furthermore, traffic-induced turbulence σ_{wt} and wind-driven turbulence σ_{ww} both play essential roles in determining the total turbulence level σ_w [127]. For instance, Solazzo et al. [145] found a strong correlation between σ_w, the ambient wind speed U_{ref}, and σ_{wt}, which was expressed as follows:

$$\sigma_w = (\sigma_{ww}^2 + \sigma_{wt}^2)^{1/2} = [(C_a \times U_{ref})^2 + \sigma_{wt}^2]^{1/2}, \quad (1)$$

where C_a is typically 0.1. Zhang et al. [146] determined that the ratio of σ_{wt} and U_{ref} (i.e., σ_{wt}/ U_{ref}) described the relative effect of TPT and wind-driven turbulence on pollutant dispersion in the urban context. Furthermore, Rastetter [147] reported that the effects of moving vehicles and wind speed impacted the pollutant concentration equally.

At a specific traffic density, the same ratio of V/U_{ref} provided the same concentration values, where V denotes the average speed of the vehicles. Similarly, Kastner-Klein et al. [131] pointed out that the in-canyon concentration changed linearly with $a^{1/3}$ V/U_{ref}, where a represents the traffic density.

Consequently, it can be deduced that the influences of the inflow conditions (e.g., wind speed), thermal effects (e.g., thermal intensity), and moving vehicles are of the same order.

3.5 Summary of mechanical measures

Table 8 (summarized from Tables 1-7) compares the influences of all mechanical measures on the pollutant concentration for the same urban configuration, emission type, and measurement position. Interestingly, all three mechanical measures (inflow wind conditions, thermal effects, and vehicular motions) significantly impact pollutant dispersion in the urban context, and their influences on the pollutant concentration are of the same order. This is also in line with the analysis of section 3.4. Generally, the influence of all three mechanical measures is significant and should not be ignored by urban planners and architects.

Table 8 Comparison of the influences of different mechanical measures on the pollutant concentration

Ref.	Sensitivity analysis	Urban configuration	Emission type	Position of measurement	Variation of concentration
[46]	a1	S (H/W = 1)	Passive gaseous pollutant	Ped. Level	44%
[58]	a2	S ($H/W \approx$ 1)	Passive gaseous pollutant	Ped. Level	42%
[70]	a3	S (H/W = 1)	Passive gaseous pollutant	Ped. Level	50%
[78]	a4	S (H/W = 1)	Passive gaseous pollutant	Ped. Level	86%
[95]	b1	S (H/W = 1)	Passive gaseous pollutant	Ped. Level	90%
[106]	b2	S (H/W = 1)	Passive gaseous pollutant	Ped. Level	80%
[131]	c1	S (H/W = 1)	Passive gaseous pollutant	Ped. Level	42%
[139]	c2	S (H/W = 0.8)	Passive gaseous pollutant	Ped. Level	44%

Sensitivity analysis: a1= Inflow wind speed, a2= Time-varying inflow, a3= Inflow turbulent fluctuation, a4= Inflow wind direction, b1 = Thermal stratification, b2 = Thermal position, c1 = Vehicle speed, c2 = Traffic composition, c3= Vehicle shape. **Urban configuration:** S= Street canyon, H/W = Height aspect ratio (building height/ street width); **Position**: Ped. Level = Pedestrian level

4. Effects of urban morphology

A literature review indicates that the urban wind environment has high spatial variation and strongly depends on the characteristics of the urban texture features

[19,148–153]. Once traffic emissions are discharged into the atmosphere, the distribution of air pollution is considerably affected by the urban morphology [154–158]. Accordingly, it is essential to identify which urban morphology characteristics have a prominent influence on the ventilation and corresponding pollutant dispersion [159].

According to different geometries, the study regions can be divided into four lengths or scales: the regional scale (up to 100 or 200 km), city-scale (up to 10 or 20 km), neighborhood scale (up to 1 or 2 km), and street scale (less than 100–200 m) [160,161]. It is noteworthy that health impacts are evident on a local scale, although the average data on a city scale may meet the regulatory standards [162]. The reason is that average values at the urban or regional scales cannot be used for the control of local air quality due to a lack of information on the microenvironment (e.g., on-site meteorology, thermal environment, and traffic flows) and a low resolution for the calculation of urban morphology features [163]. Therefore, this section focuses on understanding the influence of urban morphology at the neighborhood and street scales. At the neighborhood scale, we identify two levels of urban morphology based on the classification of Yang and Fu [164]. The first level is the urban density. The second level represents the urban spatial characteristics, including urban heterogeneity and the degree of enclosure. At the street scale, a review is conducted of studies on the height aspect ratio, building opening/separation, and the influence of viaducts.

4.1 Neighborhood scale

4.1.1 Effects of urban density

First, we determine the correlation between urban density and pollutant dispersion. Urban density is more than just a ratio that affects the resource efficiency or liveability of cities. It also considerably impacts the pollutant distribution in the urban context. Thus, there are apparent conflicts between land use and outdoor air quality. In this section, we assess the potential link between urban planar density (the proportion of land area that can be utilized for development) and frontal area density (FAD) on the

one hand (the impact of the vertical surface) and urban outdoor air quality on the other hand.

4.1.1.2 Planar urban density

Typically, planar urban density at the neighborhood scale is described by the building coverage ratio (BCR) (also known as planar area density λ_p [165]), which is the ratio of the buildings' footprint area to the total area under consideration [166] (Fig. 10 (a)). Kubota et al. [167] found a negative linear correlation between BCR (%) and R_u (the average pedestrian-level wind speed ratio, which is equal to the ratio of local/reference wind speed) with R^2=0.87: R_u= –0.01*BCR+0.8 (or 0.56) (Fig. 10 (b)). With an increase in BCR (10%-35%), the R_u decreased by about 35.7%. This result may be attributable to a reduction in the pressure difference between buildings, which limits the ventilation potential in areas of high urban density [168–170]. Therefore, it follows that there is a positive relationship between the mean age of air (Age, which is defined as the time required for rural air to reach a given location after entering an urban area; a larger Age represents poorer air quality) and BCR: Age= 411.92*BCR+83.08 [170]. Likewise, Di Sabatino et al. [171] found that the in-canyon maximum CO concentration increased from 700 to 5000 μg/m^3 when the BCR increased from 6.25% to 44%. Similarly, Buccolieri et al. [168] reported that the maximum normalized Age increased from 6 to 21 as the BCR increased from 25% to 56% (Fig. 10 (c)). Interestingly, an increase in the BCR results in increased turbulence at the rooftop [148]. However, an increase in the turbulence level did not offset the significant reduction in ventilation potential. Accordingly, this result provides convincing evidence that pollutant dispersion is mainly affected by the mean flow, which changes with a change in the BCR.

4.1.1.2 Vertical urban density

Srebric et al. [172] pointed out that it is more practical to classify urban neighborhoods using vertical urban density for the most densely populated cities, e.g., Singapore, Hong Kong, and Manhattan in New York City. The reason is that the vertical

urban density reflects the height blockage in dense areas.

Usually, the FAD is used to describe the vertical urban density at the neighborhood scale (Fig. 10 (d)), since it is the ratio of the frontal area of buildings exposed to the wind to the total area under consideration [173,174]. Yang et al. [169] reported that the wind velocity increased with an increase in the FAD in the main street canyons (streamwise canyons) due to a strong "Venturi effect", but it decreased gradually in the secondary street canyons (spanwise canyons). Thus, as illustrated in Fig. 10 (e), the average wind speed ratio at the pedestrian level decreased with an increase in the FAD, causing the accumulation of pollutants. A similar phenomenon was also observed by Li et al. [175] and Bentham and Britter [176]. Accordingly, there is a positive correlation between the FAD and pollutant concentration for urban arrays, as shown in Fig. 10 (f). A nearly four-fold increase in the FAD resulted in an approximately 50% increase in Age (worse air quality) at the pedestrian level [169]. Moreover, Mei et al. [177] investigated wind-driven natural ventilation in a set of urban arrays with a range of the FAD from 10% to 80%. The results indicated that a change in the FAD significantly altered the flow patterns, particularly in secondary canyons. With an increase in the FAD, the axis of the secondary-canyon vortex changed from horizontal to vertical, causing a weaker air exchange at the rooftop. Hence, the maximum Age in the center area increased by two times with increasing FAD. Interestingly, once the FAD exceeded 0.4, the pollutant removal potential was quite weak. Likewise, Shi et al. [178] found that an increase in the FAD resulted in the reduction of the horizontal permeability of urban ventilation, further impeding the dispersion of airborne pollution.

In effect, the FAD might not be uniform in the vertical direction. As noted by Ng et al. [179], the FAD in the lower layers of urban areas in Hong Kong was marginally higher than in higher layers due to the existence of a podium. Thus, the FAD was divided into three layers according to the height (podium layer (0-15 m), building layer (15-60 m), and urban canopy layer (0-60 m)). Shi et al. [7] used this classification and conducted a four-mouth monitoring campaign in Hong Kong; it was found that the FAD

of the podium layer had the most significant positive correlation with the PM2.5 concentration.

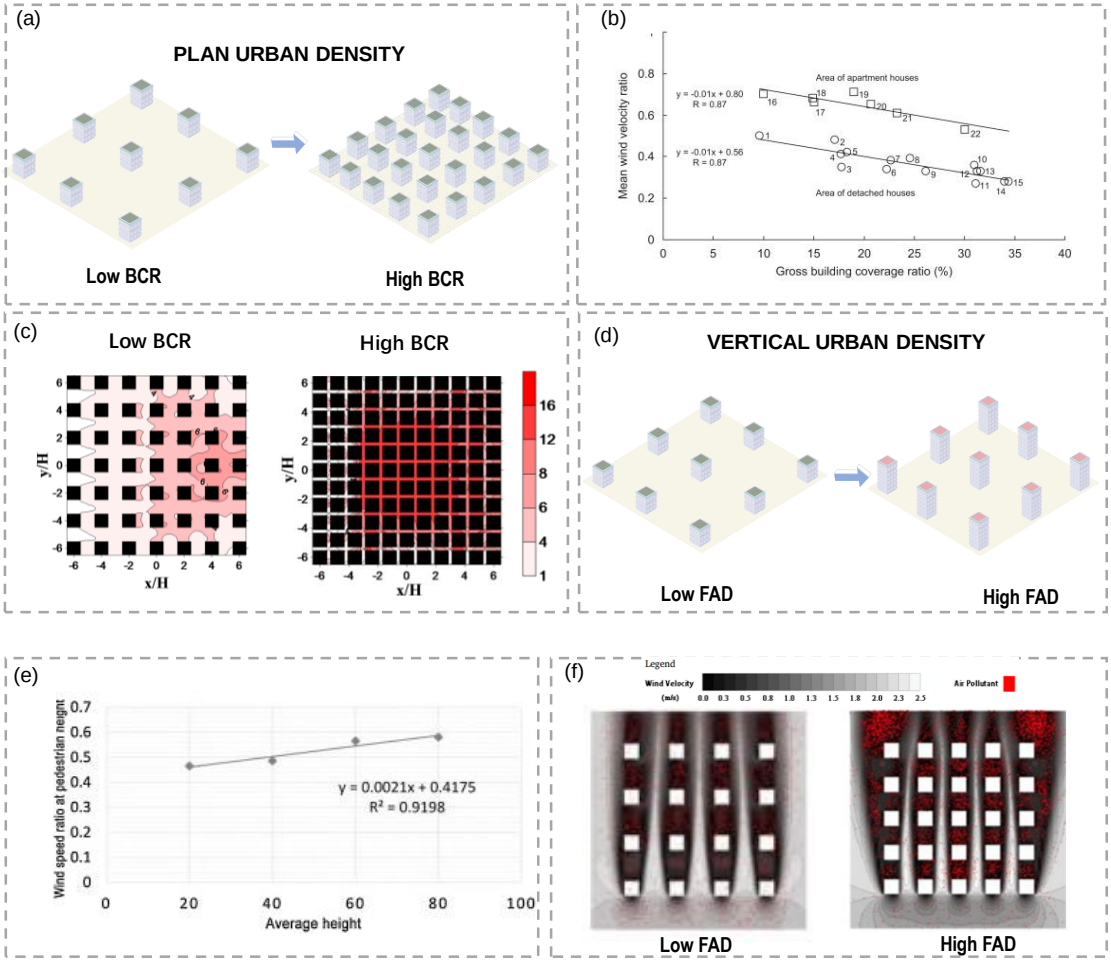

Fig. 10 (a) Illustrations of planar urban density; (b) relationship between planar building density and mean wind velocity ratio [167]; (c) normalized mean age of air at the pedestrian level for different planar building densities [168]; (d) illustrations of vertical urban density; (e) correlation of wind speed ratio and average height [169]; (f) simulation results of the wind environment and air pollution flow for different FAD values [169].

Table 9 Overview of studies on the effect of urban density

Ref.	Focus	Sensitivity analysis	Study approach	Remarks
[169]	a, c	1, 2	CFD (V)	A negative linear correlation was observed between BCR (%) and mean wind speed; a nearly four-fold increase in the FAD resulted in an approximately 50% increase in Age (worse air quality) at the pedestrian level
[168]	a, c	1	CFD (V)	The maximum normalized Age increased from 6 to 21 as the BCR increased from 25% to 56%
[177]	a	2	CFD (V)	With an increase in the FAD, the axis of the secondary-canyon vortex changed from horizontal to vertical, causing a weaker air exchange at the rooftop
[7]	a, c	2	FM	The FAD of the podium layer had the most significant positive correlation with the PM2.5 concentration

Focus: a = Mean flow, b = Turbulence, and c = Pollutant; **Sensitivity analysis:** 1= Planar urban density, and 2= vertical urban density; **Study approach:** WT = Wind tunnel measurements, FM = Field measurements, CFD (V) = CFD with validation, and CFD (NO) = CFD without validation.

4.1.2 Effects of urban heterogeneity

In urban arrays, the building height and the layout of buildings are rarely uniform [157], as shown in Fig. 11 (a) and (d). Furthermore, the irregular building geometry and non-uniform building spacing, height, and layout cause complex flow and turbulent characteristics. For instance, the variations in the building height result in a substantial velocity fluctuation at the top shear layer, promoting the dilution of pollutants from the lower areas of the street canyons. Therefore, it is crucial to obtain an in-depth understanding of the influence of urban heterogeneity and utilize the heterogeneity to improve pollutant dispersion.

4.1.2.1 Planar urban heterogeneity

The staggered layout of buildings is a typical non-uniform urban configuration, resulting in planar heterogeneity [180]. In contrast to the investigation of the flow characteristics of regularly aligned arrays of buildings, the flow characteristics of a staggered layout have not been considered in detail in the literature.

Bady et al. [181] observed that the flow structures of aligned and staggered layouts were fundamentally different. Under perpendicular wind, the staggered arrays diverted airflow to downstream obstacles, whereas the aligned arrays caused a channeling flow. Accordingly, higher passive gaseous pollutant concentration was found in the staggered arrays due to their poorer ability to remove pollutants under this wind direction. However, for an oblique wind (θ =45°), the staggered array yielded

better ventilation potential because the aligned blocks produced more circular vortices in this wind direction. Differently, Lin et al. [82] stated that the staggered arrays always yielded a lower ventilation efficiency than the aligned arrays under any wind direction ($45° < \theta < 90°$) (Fig. 11(b)). The possible explanation might be the different distances between two rows of building arrays (different planar building density). In other words, an improvement in the ventilation provided by the staggered layout was strongly spatially dependent [182]. Also, Cheung and Liu [183] tested the sensitivity of urban ventilation to different degrees of building shifts in staggered layouts. With a suitable building shift, the staggered layout could improve the ventilation rate two-fold compared with the aligned one. Meanwhile, it was found that the influence of the staggered layout could be weakened by a larger building separation. Yazid et al. [184] confirmed this result. The interference effect of the building shift was investigated for a group of buildings with different planar urban densities. As shown in Fig. 11 (c), the reduction in the passive gaseous pollutant (CO) concentration was more significant for closely packed buildings for aligned buildings and staggered layout buildings.

4.1.2.2 Vertical urban heterogeneity

Vertical urban heterogeneity is the result of differences in building heights. Cheng and Castro [185] demonstrated that the non-uniformity of the building height notably enhanced the vertical momentum transport compared with the uniform height model. Similarly, Hang and Li [186] pointed out that the ventilation of secondary streets benefited from a variation in the building height due to the stronger vertical mean flow at the rooftop. Likewise, Antoniou et al. [187] investigated outdoor urban ventilation in a real complex urban area. The results revealed that an increase in the building height in the area improved the breathability level at the pedestrian level. Accordingly, Hang et al. [188] concluded that suitable building height configurations improved the breathability level in high-rise urban areas.

Interestingly, Ishida et al. [189] argued that non-uniform building height resulted in improved overall dissipation of total energy, hence deteriorating the ventilation

performance, although an increase in the TKE was observed (Fig. 11(f)). Moreover, Lin et al. [82] observed that building height differentials weakened horizontal flows along the street, although the vertical air exchange was improved. Therefore, it is difficult to conclude whether a non-uniform building height improves urban ventilation or not. This conclusion is in line with the results of Chen et al. [190], Wang et al. [191,192]. Chen et al. [190] analyzed the ventilation potential in a group of urban arrays with six standard deviations of the height. The non-uniformity in the building height caused an approximately 40% decrease in the vertical air exchange but increased the horizontal air exchange by up to 40%. Thus, similar to the influences of urban planar heterogeneity, the effects of the building height are also strongly spatially dependent. Wang et al. [191,192] investigated the combined effects of urban vertical heterogeneity and planar density on ventilation performance. As shown in Fig. 11 (e) for the case of H=30 m as an example, the median wind velocity ratio of buildings with a non-uniform height was nearly 0.1 higher than their uniform height counterpart when the planar urban density was low (X1). However, when the planar urban density was high (X2), the median value was lower for buildings with a non-uniform height.

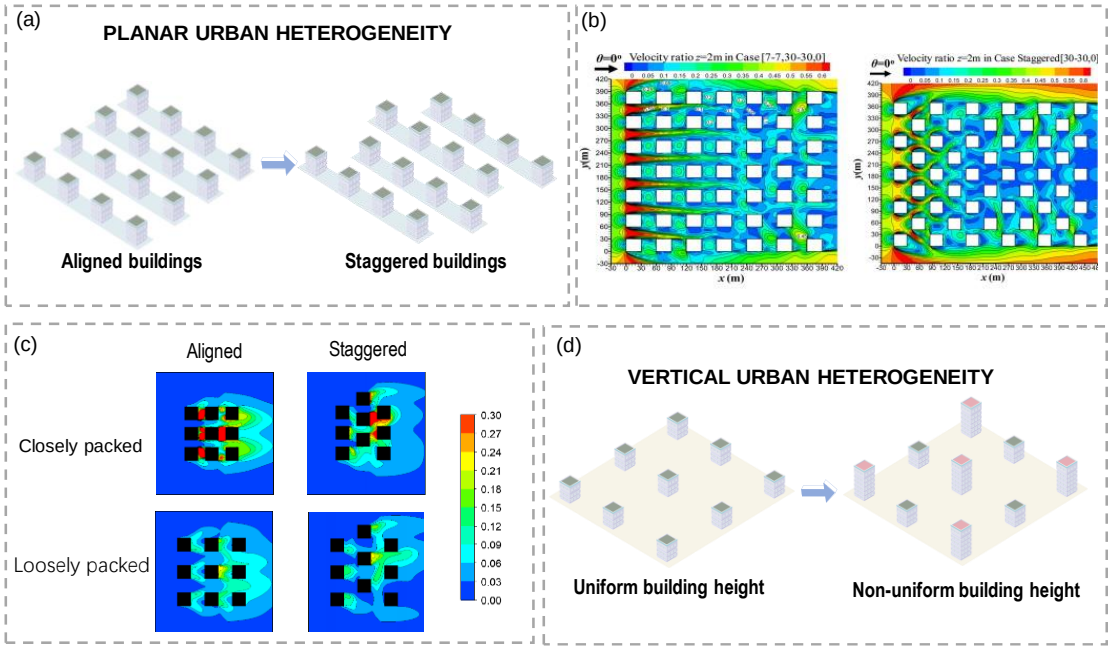

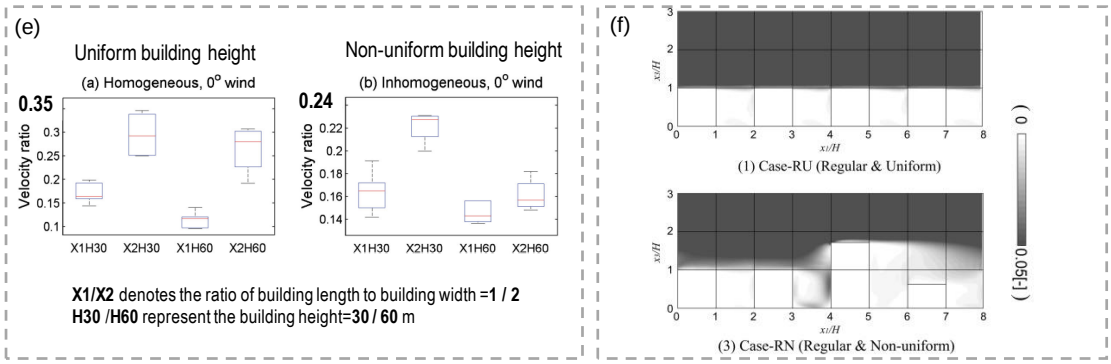

Fig. 11 (a) Illustrations of planar urban heterogeneity; (b) contours of the velocity ratio for z = 2 m for different planar urban heterogeneities [82]; (c) contours of the concentration near the ground for different planar urban heterogeneities [184]; (d) illustrations of vertical urban heterogeneity; (e) ventilation performance associated with the building aspect ratio and vertical urban heterogeneity [192]; (f) vertical distributions of the dimensionless mean TKE [189]

Table 10 Overview of studies on the effect of urban heterogeneity

Ref.	Focus	Sensitivity analysis	Study approach	Remarks
[82]	a, c	1, 2	CFD (V)	The staggered arrays always yielded a lower ventilation efficiency than the aligned arrays one for any wind direction (45° < θ < 90°); building height differentials weakened horizontal flows along the street, although the vertical air exchange was improved.
[183]	a	1	CFD (V)	With a suitable building shift, the staggered layout improved the ventilation rate two-fold compared with the aligned one.
[184]	a, c	1	CFD (V)	The reduction in the pollutant concentration was more significant for closely packed buildings than for aligned buildings and staggered layout buildings.
[185]	a	2	WT	Non-uniformity of the building height notably enhanced the vertical momentum transport compared with the uniform height model
[190]	a, c	2	CFD (V)	The non-uniformity in the building height caused an approximately 40% decrease in the vertical air exchange but increased the horizontal air exchange by up to 40%.

Focus: a = Mean flow, b = Turbulence, and c = Pollutant; **Sensitivity analysis:** 1= Planar urban heterogeneity, and 2= vertical urban heterogeneity; **Study approach:** WT = Wind tunnel measurements, FM = Field measurements, CFD (V) = CFD with validation, and CFD (NO) = CFD without validation.

4.1.3 Effects of urban enclosure degree

As stated by Yang and Fu [164], the degree of the urban enclosure is a crucial parameter affecting the openness of the urban architectural space (Fig. 12 (a)). A smaller degree of the enclosure is related to greater openness of this space, and vice versa. Cui et al. [193] pointed out that a larger degree of enclosure provided more private space but also caused some weak winds. Yang et al. [169] defined the planar

ED as the ratio of the sum of the side length of all the outer buildings along the roads to the boundary length of the buildings. The results indicated a strong negative correlation between the ED and the pedestrian-level wind velocity ratio R_u: R_u= −1.065×ED+0.987. As the ED increased from 0.4 to 0.7, the R_u decreased by nearly 54%. The reason is that it is more difficult for ambient wind to reach the inside of the area with an increase in the ED. Therefore, the passive gaseous pollutant concentration increased with increasing ED (Fig. 12(b)). Iqbal and Chan [194] investigated the wind circulation in four building configurations with different planar enclosure degrees (square, U-, L-, and I- shape). The results revealed that the building configuration with a lower ED (L- and I- shape) had a higher ventilation potential. Similarly, Cui et al. [195] compared the pedestrian level wind environment (PLWE) of semi-closed U-type street canyons (higher ED) with that of regular parallel canyons (lower ED). The results suggested that the U-type canyons provided a worse PLWE both inside and near the canyons, particularly under parallel wind. Thus, a suitable ED of long street canyons is essential [33]. On the other hand, Yang et al. [148] quantified the "degree of planar enclosure" using the sky view factor (SVF). The results showed that an increase in the SVF by 10% (increased openness) caused a 7-8% decrease in the pedestrian-level wind speed.

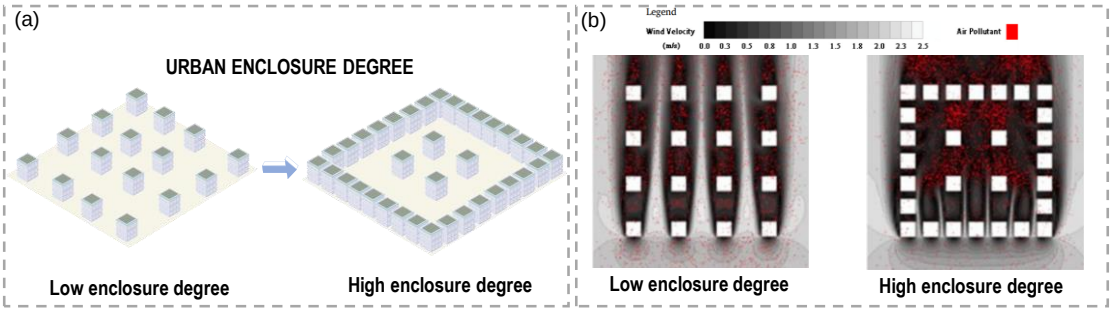

Fig. 12 (a) Illustrations of the urban enclosure degree; (b) simulation results of the wind environment and air pollution flow for different urban enclosure degrees [169].

Table 11 Overview of studies on the effect of urban enclosure

Ref.	Focus	Study approach	Remarks
[193]	a	CFD (V)	A larger degree of enclosure provided more private space but also caused some weak winds
[148]	a	FM	The "degree of planar enclosure" was assessed using the sky view factor (SVF); an increase in the SVF of 10% (increased openness) caused a 7-8% decrease in the pedestrian-level wind speed.
[169]	a, c	CFD (V)	As the ED increased from 0.4 to 0.7, the wind velocity ratio decreased by nearly 54%, and the pollutant concentration increased.

Focus: a = Mean flow, b = Turbulence, and c = Pollutant; **Study approach:** WT = Wind tunnel measurements, FM = Field measurements, CFD (V) = CFD with validation, and CFD (NO) = CFD without validation.

4.2 Street scale

4.2.1 Effects of the height aspect ratio

The height aspect ratio (*H/W*, the ratio of the building height to the street width) was used to parameterize the canyon geometry and predict the ventilation at the street scale [196] (Fig. 13(a)). Oke [197] found that when the ambient wind was perpendicular to the street axis, three distinct flow regimes were observed depending on the aspect ratio: isolated flow ($H/W < 0.3$), wake interference flow ($0.3 < H/W < 0.7$), and skimming flow ($H/W > 0.7$) (Fig. 13(b)). Xie et al. [198] observed two counter-rotating vortices in the canyon with $H/W = 2$. The ventilation was worse in deeper canyons ($H/W = 3$-5), even when 3-5 vertically aligned vortices occurred [82]. Wen et al. [199], Li et al. [200] and Zhang et al. [201] found that the wind speed in the lower space of the canyons decreased substantially with increasing *H/W* (Fig. 13(c)). Also, Zhang et al. [202] determined that the pedestrian-level wind speed dropped by 1-2 orders as the *H/W* increased from 1 to 5. Due to the worse ventilation, the spatial personal intake fraction (*P_IF*) of passive pollutants (CO) increased by 1-2 orders [202]. Likewise, the mean concentration of reactive pollutants (NO_x) increased by nearly three times [201] (Fig. 13(d)). Interestingly, Liu et al. [203] found that the air quality in shallow canyons with $H/W = 0.2$-0.5 was relatively poor compared to that in deeper canyons ($H/W = 2.5$). The possible reason could be the re-entrainment of air pollutants through the top shear layer.

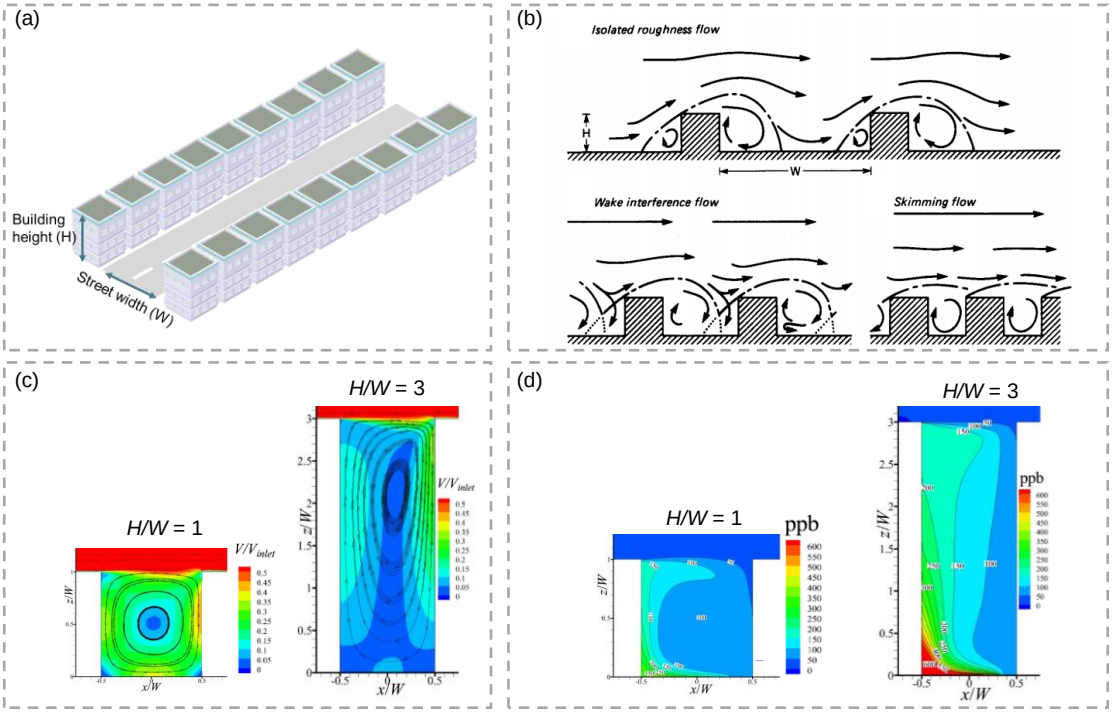

Fig. 13 (a) Illustrations of the height aspect ratio of the street canyon; (b) the flow regimes associated with airflow over building arrays with increasing *H/W* [197]; (c) streamline and normalized velocity for different *H/W* [201]; (d) C_{NO} (ppb) for different *H/W* [201]

Table 12 Overview of studies on the effect of height aspect ratio

Ref.	Focus	Study approach	Remarks
[192]	a, c	CFD (V)	The wind speed in the lower part of the canyons decreased substantially with increasing H/W
[202]	a, c	CFD (V)	The pedestrian-level wind speed dropped by 1-2 orders of magnitude as the H/W increased from 1 to 5; the spatial personal intake fraction (P_IF) of passive pollutants increased by 1-2 orders of magnitude
[201]	a, c	CFD (V)	The mean concentration of the reactive pollutants increased by nearly three times

Focus: a = Mean flow, b = Turbulence, and c = Pollutant; **Study approach:** WT = Wind tunnel measurements, FM = Field measurements, CFD (V) = CFD with validation, and CFD (NO) = CFD without validation.

4.2.2 Effects of building opening/ separation

Changing the building opening on the building surface is an effective solution to improve the PLWE without losing land [204]. As explained by Du and Mak [205], this building opening resulted in a significant increase in the permeability of a single building (Fig. 14(a)). An et al. [206] pointed out that the degree of building opening should be at least 20% to maintain good ventilation for all canyons (Fig. 14(b)). Permeabilities of 10% to 15% only reduced the passive gaseous pollutant concentration

in street canyons immediately downwind, but more pollutants were accumulated in canyons further downwind (Fig. 14(c)). Moreover, Yang et al. [207] investigated the influence of the window-opening percentage (WOP) on in-canyon ventilation. The results indicated that an increase in the WOP from 0% to 10% resulted in a 27% decrease in the passive gaseous pollutant concentration. Also, the effects of the WOP weaken with an increase in the *H/W*.

On the other hand, the Building Department in Hong Kong identified building separation as one of the key urban design elements to achieve better air ventilation in urban areas [208]. Building separation was adopted to create an intervening space and separate the long street canyon into a series of short canyons to allow more fresh air into the canyon (Fig. 14(d)). The degree of building separation is defined as the ratio of the length of the building separation *S* to the length of the street *L* [209]. Fan et al. [210] examined the influence of six types of building separation on the ventilation potential. The results revealed that a 10% value for building separation was sufficient to increase the pedestrian-level wind speed. Ng and Chau [209] highlighted the significant relationship between building separation and in-canyon ventilation. It was demonstrated that the ventilation potential was substantially improved by introducing building separations, which yielded a more than 80% decrease in the mean passive gaseous pollutant (CO) exposure in a canyon with *H/W* =4 under perpendicular wind (Fig. 14(e)). Interestingly, a significant reduction in the pollutant concentration occurred by increasing the degree of building separation from 0% to 10%, whereas the concentration changed only slightly by changing the degree of building separation from 10% to 35%. Conversely, under parallel wind, building separation increased the pollutant concentration. Similarly, Shen et al. [211] confirmed that, under parallel approaching wind, higher values of street continuity and a spatial closure ratio caused a stronger channeling flow, improving the local air quality (Fig. 14(f)).

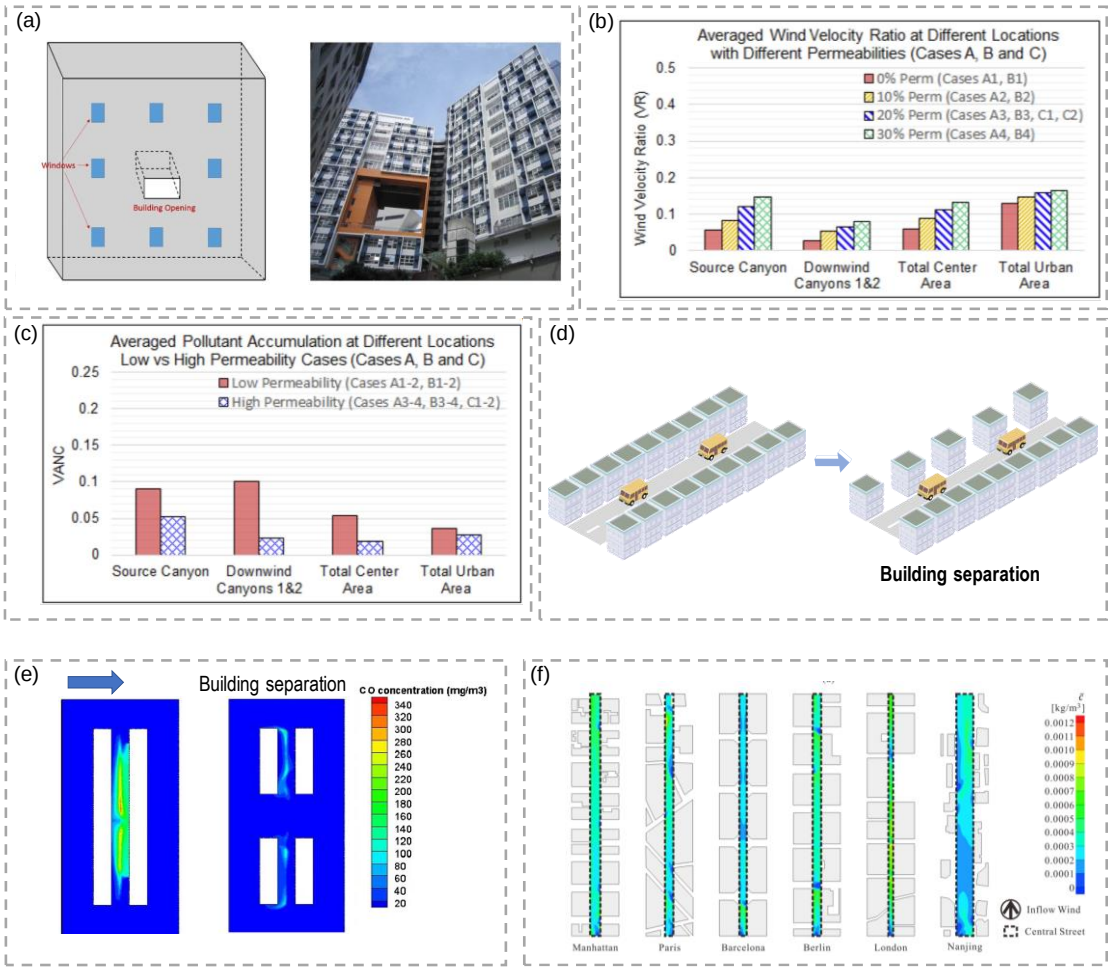

Fig. 14 (a) Schematic diagram of a building opening and photo of a building with an opening [205]; (b) wind velocity ratio for different permeabilities in different focus areas [206]; (c) comparison of volume-averaged normalized concentration between cases with low permeability and high permeability [206]; (d) schematic diagram of building separation; (e) comparison of the CO concentration between cases with building separation and without separation under perpendicular wind [209]; (f) comparison of the CO concentration of different realistic street canyons under parallel wind [211]

Table 13 Overview of studies on the effects of building opening/ separation

Ref.	Focus	Study approach	Remarks
[206]	a, c	CFD (V)	The degree of building opening should be at least 20% to maintain good ventilation for all canyons.
[207]	a, c	CFD (V)	An increase in the WOP from 0% to 10% resulted in a 27% decrease in the pollutant concentration.
[209]	a, c	CFD (V)	Ventilation potential was substantially improved by introducing building separation, which yielded a more than 80% decrease in the mean pollutant exposure in a canyon with H/W =4 under perpendicular wind.
[211]	a, c	CFD (V)	Under parallel approaching wind, higher values of street continuity and a spatial closure ratio caused a stronger channeling flow, improving the local air quality

Focus: a = Mean flow, b = Turbulence, and c = Pollutant; **Study approach:** WT = Wind tunnel measurements, FM = Field measurements, CFD (V) = CFD with validation, and CFD (NO) = CFD without validation.

4.2.3 Effects of viaducts

The existence of a viaduct in the canyon reduces the ventilation (Fig. 15(a)), although it helps to alleviate traffic congestion in peak periods [212]. The reduction in ventilation occurs because viaducts markedly alter the in-canyon flow characteristics. Besides, the influence of the viaduct was strongly dependent on its geometric features (e.g., the height and width of the viaduct and the installation of noise barriers) and that of the street canyons (e.g., *H/W*). Hang et al. [213] found that in a canyon with *H/W* =1, the principal main vortex could be divided into several vortices above and beneath the viaduct (Fig. 15(b)). Thus, Zhi et al. [214] reported that this viaduct weakened the recirculation of the main vortex, the in-canyon ventilation deteriorated, and the average mass concentration of pollutants (PM10, PM2.5, and PM1) increased by up to 15%, which was confirmed by Hang et al. [213] (Fig. 15(c)). Duan et al. [215] observed that the mean flow decelerated below elevated walkways and increased the concentration by up to 20%, although the level of TKE around the elevated walkways was improved. Furthermore, Zhang et al. [202] investigated the influence of viaducts on a series of canyons with different values of *H/W*. The viaduct, which had a fixed height, resulted in a nearly three-fold increase in the volumetric <*P_IF*> in a deep canyon (*H/W* =5) but only slightly influenced the <*P_IF*> in a relatively low canyon (*H/W* =1 and 3). The reason is that the blockage effect of the viaduct significantly affects the pollutant concentration below the viaduct when the advection effect is weak. Huang and Zhou [216] investigated the influence of the height of the viaduct. It was found that the in-

canyon wind speed was the lowest when the viaduct was as high as the building height; this configuration resulted in the highest pollutant concentration. As further explained by Ding et al. [217], a viaduct with the same height as the building produced a series of small vortices in the location of the main vortex near the leeward side. The viaduct acted as a "cap" to prevent ventilation in the canyons (Fig. 15(d)). Accordingly, the maximum passive gaseous pollutant concentration increased by approximately one order. However, the ventilation returned to the initial flow condition when the viaduct height was more than 1.2 times the building height. Interestingly, if only the elevated pollutant source above the viaduct was considered instead of the ground-level source, Hang et al. [218] and He et al. [219] found that the viaducts reduced the overall indoor pollutant exposure. The possible reason is that the weaker circulation above the viaduct caused the accumulation and deposition of pollutants onto the viaduct surface.

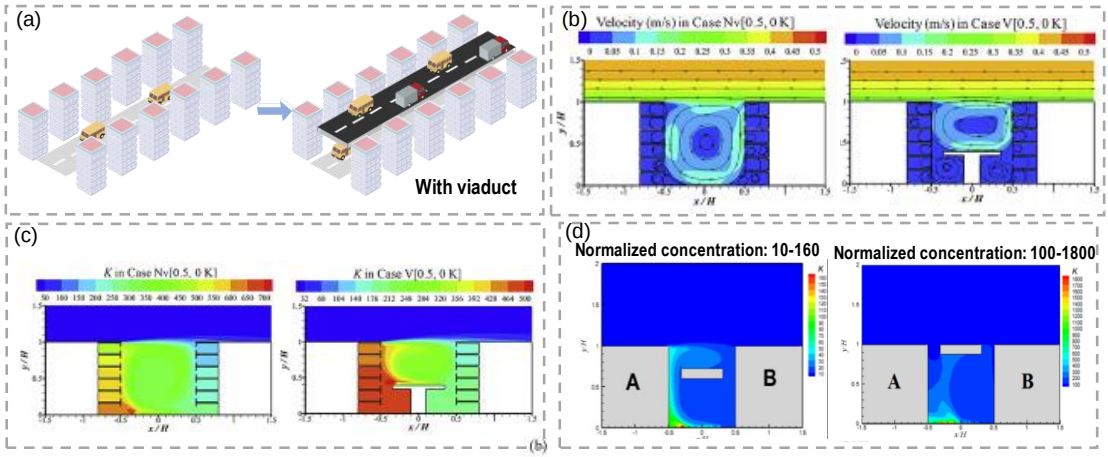

Fig. 15 (a) Schematic diagram of a street canyon with a viaduct; (b) streamlines and velocity magnitude in street canyons [213]; (c) contours of the pollutant concentration in street canyons [213]; (d) contours of the pollutant concentration in street canyons with viaducts of different heights [217].

Table 14 Overview of studies on effects of the viaduct

Ref.	Focus	Study approach	Remarks
[213]	a, c	CFD (V)	In a canyon with H/W =1, the principal main vortex could be divided into several vortices above and beneath the viaduct
[214]	a, c	CFD (V)	The viaduct, which had a fixed height, resulted in a nearly three-fold increase in the volumetric <P_IF> in a deep canyon (H/W =5) but only slightly influenced the <P_IF> in a relatively low canyon (H/W =1 and 3)
[215]	a, b	CFD (V)	The level of TKE around the elevated walkways was improved
[218]	a, c	CFD (V)	If only the elevated pollutant source above the viaduct was considered instead of the ground-level source, the viaducts reduced the overall indoor pollutant exposure

Focus: a = Mean flow, b = Turbulence, and c = Pollutant; **Study approach:** WT = Wind tunnel measurements, FM = Field measurements, CFD (V) = CFD with validation, and CFD (NO) = CFD without validation.

4.4 Summary of urban morphology

In summary, as shown in Tables 9-14, the effects of urban morphology on pollutant dispersion can be divided into two scales (neighborhood and street scale) and are dependent on three key parameters at each scale, i.e., the urban density, urban heterogeneity, and urban enclosure degree at the neighborhood scale, and the height aspect ratio, building opening/separation, and viaduct at the street scale.

At the neighborhood scale, higher planar and vertical urban densities decrease the air recirculation in the urban canopy, causing higher pollutant concentrations in urban areas, except in extreme situations. This result was expected. Notably, a decrease in the planar and vertical urban densities reduced the pollutant concentrations by 50-86%. However, the effects of urban heterogeneity in the planar direction (staggered layout versus aligned layout) or vertical direction (building height variations) are strongly spatially dependent. It is difficult to conclude whether urban heterogeneity improves the overall urban ventilation or not. Nonetheless, an optimal heterogeneity to achieve good air quality for specific spatial characteristics was reported. The pollutant concentration was reduced by nearly 83% and 75% with changes in the planar and vertical heterogeneities, respectively, by using an appropriate design. Although no quantitative results were reported for the effect of the urban enclosure degree on pollutant reduction, we can infer changes in the pollutant concentration from changes in the ventilation. An increase in the urban enclosure degree can cause an almost 54% decrease in the local wind speed.

At the street scale, the spatial pollutant concentration increased by 1-2 orders of magnitude as the height aspect ratio increased from 1 to 5. Thus, the air quality of deep street canyons has to be considered. The degree of building opening should be at least 20% to maintain good ventilation in urban areas. Similarly, the degree of building separation should not be less than 10%. On the other hand, in some cases, the existence of a viaduct caused a nearly 15% increase in pollutant concentration. The air quality was worse when the viaduct was as high as the buildings.

5. Conclusion

Deteriorating outdoor air quality significantly affects public health and may cause substantial economical loss. Therefore, it is essential to improve outdoor air quality. This paper evaluated the effects of influential factors on pollutant dispersion and discussed their basic underlying mechanisms (affected by mean flow and turbulence). Generally, the reviewed papers were categorized into two groups: (i) the utilization of mechanical factors, including forced convection by ambient wind, natural convection by solar radiation, and traffic-induced convection due to traffic movement; (ii) the improvement of the capacity to reduce air pollution by modifying the urban morphology, including the urban density, urban heterogeneity, and urban enclosure degree at the neighborhood scale, and the height aspect ratio, building opening, building separation, and viaducts at the street scale. The following conclusions can be drawn from the literature review:

(1) The three mechanical measures (inflow wind condition, thermal effects, and vehicular motions) have similar levels of influence on the dispersion and distribution of pollutants within the urban context. For similar urban configurations, emission types, and measurement positions, the mechanical measures caused a significant reduction in the pollutant concentration (a reduction of 42% to 90%). The influence of the three factors is significant and should not be ignored by urban planners and architects.

(2) Similarly, the six morphological parameters (urban density, heterogeneity, and enclosure degree at the neighborhood scale, and the height aspect ratio, building

opening, building separation, and viaducts at the street scale) played significant roles in determining the dispersion of air pollutants. At the neighborhood scale, the frontal and planar urban density and enclosure degree should be as small as possible. By decreasing the two densities and the enclosure degree, the pollutant concentration was reduced by up to 86%. It is difficult to conclude whether urban heterogeneity in the planar direction (staggered layout versus aligned layout) or vertical direction (building height variations) had adverse or positive effects on urban ventilation since planar and vertical heterogeneity are strongly spatially dependent. For urban areas with a high planar density, an appropriate staggered urban layout or non-uniform building height should be considered to improve the local wind environment. At the street scale, the pollutant concentration increased by 1-2 orders of magnitude as the height aspect ratio increased from 1 to 5. Thus, the air quality of the deep street canyon needs to be considered. The degree of building opening should be at least 20% to maintain good ventilation in urban areas. Similarly, the degree of building separation should not be less than 10%. Also, the existence of a viaduct caused a nearly 15% increase in pollutant concentration. The air quality worsened when the viaduct was as high as the buildings.

In summary, this paper provided a comprehensive and systematic review of the effects of different influential factors on pollutant dispersion. Detailed quantifications of the reduction potential of different factors were reported. Accordingly, this study is beneficial for urban planners and architects who are responsible for decision-making.

Acknowledgments

This study was financially supported by the National Natural Science Foundation of China (Grant No. 51778511), the Hubei Provincial Natural Science Foundation of China (Grant No. 2018CFA029), the Key Project of ESI Discipline Development of Wuhan University of Technology (WUT Grant No. 2017001), and the Fundamental Research Funds for the Central Universities (WUT Grant No. 2019IVB082).

REFERENCE

[1] S. Grimmond, Urbanization and global environmental change: local effects of urban warming, Geogr. J. 173 (2007) 83–88.

[2] C. Peng, T. Ming, J. gui, Y. Tao, Z. Peng, Numerical analysis on the thermal environment of an old city district during urban renewal, Energy Build. 89 (2015) 18–31. doi:https://doi.org/10.1016/j.enbuild.2014.12.023.
[3] R. Rückerl, A. Schneider, S. Breitner, J. Cyrys, A. Peters, Health effects of particulate air pollution: a review of epidemiological evidence, Inhal. Toxicol. 23 (2011) 555–592.
[4] Y. Xia, D. Guan, X. Jiang, L. Peng, H. Schroeder, Q. Zhang, Assessment of socioeconomic costs to China's air pollution, Atmos. Environ. 139 (2016) 147–156. doi:https://doi.org/10.1016/j.atmosenv.2016.05.036.
[5] Who, Ambient (outdoor) air quality and health, WHO Media Cent. (2014).
[6] S. Zhou, R. Lin, Spatial-temporal heterogeneity of air pollution: The relationship between built environment and on-road PM2.5 at micro scale, Transp. Res. Part D Transp. Environ. 76 (2019) 305–322. doi:https://doi.org/10.1016/j.trd.2019.09.004.
[7] Y. Shi, X. Xie, J.C.-H. Fung, E. Ng, Identifying critical building morphological design factors of street-level air pollution dispersion in high-density built environment using mobile monitoring, Build. Environ. 128 (2018) 248–259. doi:https://doi.org/10.1016/j.buildenv.2017.11.043.
[8] E. Ng, Policies and technical guidelines for urban planning of high-density cities – air ventilation assessment (AVA) of Hong Kong, Build. Environ. 44 (2009) 1478–1488. doi:https://doi.org/10.1016/j.buildenv.2008.06.013.
[9] K. V Abhijith, P. Kumar, J. Gallagher, A. McNabola, R. Baldauf, F. Pilla, B. Broderick, S. Di Sabatino, B. Pulvirenti, Air pollution abatement performances of green infrastructure in open road and built-up street canyon environments – A review, Atmos. Environ. 162 (2017) 71–86. doi:https://doi.org/10.1016/j.atmosenv.2017.05.014.
[10] S. Janhäll, Review on urban vegetation and particle air pollution – Deposition and dispersion, Atmos. Environ. 105 (2015) 130–137. doi:https://doi.org/10.1016/j.atmosenv.2015.01.052.
[11] J. Gallagher, R. Baldauf, C.H. Fuller, P. Kumar, L.W. Gill, A. McNabola, Passive methods for improving air quality in the built environment: a review of porous and solid barriers, Atmos. Environ. 120 (2015) 61–70.
[12] A.W.M. Yazid, N.A.C. Sidik, S.M. Salim, K.M. Saqr, A review on the flow structure and pollutant dispersion in urban street canyons for urban planning strategies, Simulation. 90 (2014) 892–916.
[13] J. Zhong, X.-M. Cai, W.J. Bloss, Coupling dynamics and chemistry in the air pollution modelling of street canyons: A review, Environ. Pollut. 214 (2016) 690–704. doi:https://doi.org/10.1016/j.envpol.2016.04.052.
[14] M. Lateb, R.N. Meroney, M. Yataghene, H. Fellouah, F. Saleh, M.C. Boufadel, On the use of numerical modelling for near-field pollutant dispersion in urban environments− A review, Environ. Pollut. 208 (2016) 271–283.
[15] Y. Tominaga, T. Stathopoulos, CFD simulation of near-field pollutant dispersion in the urban environment: A review of current modeling techniques, Atmos. Environ. 79 (2013) 716–730.
[16] Y. Toparlar, B. Blocken, B. Maiheu, G.J.F. Van Heijst, A review on the CFD analysis of urban microclimate, Renew. Sustain. Energy Rev. 80 (2017) 1613–1640.
[17] Y. Peng, R. Buccolieri, Z. Gao, W. Ding, Indices employed for the assessment of "urban outdoor ventilation"-A review, Atmos. Environ. 223 (2020) 117211.
[18] Y. Zhao, L.W. Chew, A. Kubilay, J. Carmeliet, Isothermal and non-isothermal flow in street canyons: A review from theoretical, experimental and numerical perspectives, Build. Environ. 184 (2020) 107163.
[19] B.-J. He, L. Ding, D. Prasad, Enhancing urban ventilation performance through the development of precinct ventilation zones: A case study based on the Greater Sydney, Australia, Sustain. Cities Soc. 47 (2019) 101472.
[20] O. Coceal, T.G. Thomas, I.P. Castro, S.E. Belcher, Mean flow and turbulence statistics over groups of urban-like cubical obstacles, Boundary-Layer Meteorol. 121 (2006) 491–519.
[21] S.R. Hanna, S. Tehranian, B. Carissimo, R.W. Macdonald, R. Lohner, Comparisons of model simulations with observations of mean flow and turbulence within simple obstacle arrays, Atmos. Environ. 36 (2002) 5067–5079.
[22] J. Liu, J. Niu, Delayed detached eddy simulation of pedestrian-level wind around a building array–The potential to save computing resources, Build. Environ. 152 (2019) 28–38.

[23] J. Hang, Y. Li, R. Buccolieri, M. Sandberg, S. Di Sabatino, On the contribution of mean flow and turbulence to city breathability: the case of long streets with tall buildings, Sci. Total Environ. 416 (2012) 362–373.
[24] C.-H. Liu, D.Y.C. Leung, M.C. Barth, On the prediction of air and pollutant exchange rates in street canyons of different aspect ratios using large-eddy simulation, Atmos. Environ. 39 (2005) 1567–1574.
[25] S.E. Belcher, Mixing and transport in urban areas, Philos. Trans. R. Soc. A Math. Phys. Eng. Sci. 363 (2005) 2947–2968.
[26] F. Caton, R.E. Britter, S. Dalziel, Dispersion mechanisms in a street canyon, Atmos. Environ. 37 (2003) 693–702.
[27] A. Di Bernardino, P. Monti, G. Leuzzi, G. Querzoli, Pollutant fluxes in two-dimensional street canyons, Urban Clim. 24 (2018) 80–93.
[28] J.-J. Baik, J.-J. Kim, H.J.S. Fernando, A CFD model for simulating urban flow and dispersion, J. Appl. Meteorol. 42 (2003) 1636–1648.
[29] W.C. Cheng, C.-H. Liu, D.Y.C. Leung, Computational formulation for the evaluation of street canyon ventilation and pollutant removal performance, Atmos. Environ. 42 (2008) 9041–9051.
[30] X.-X. Li, R.E. Britter, L.K. Norford, Transport processes in and above two-dimensional urban street canyons under different stratification conditions: results from numerical simulation, Environ. Fluid Mech. 15 (2015) 399–417.
[31] P. Salizzoni, L. Soulhac, P. Mejean, Street canyon ventilation and atmospheric turbulence, Atmos. Environ. 43 (2009) 5056–5067. doi:https://doi.org/10.1016/j.atmosenv.2009.06.045.
[32] C. Gromke, B. Ruck, Influence of trees on the dispersion of pollutants in an urban street canyon—experimental investigation of the flow and concentration field, Atmos. Environ. 41 (2007) 3287–3302.
[33] S.-J. Mei, Z. Luo, F.-Y. Zhao, H.-Q. Wang, Street canyon ventilation and airborne pollutant dispersion: 2-D versus 3-D CFD simulations, Sustain. Cities Soc. 50 (2019) 101700. doi:https://doi.org/10.1016/j.scs.2019.101700.
[34] T. Michioka, H. Takimoto, A. Sato, Large-eddy simulation of pollutant removal from a three-dimensional street canyon, Boundary-Layer Meteorol. 150 (2014) 259–275.
[35] Š. Nosek, V. Fuka, L. Kukačka, Z. Kluková, Z. Jaňour, Street-canyon pollution with respect to urban-array complexity: The role of lateral and mean pollution fluxes, Build. Environ. 138 (2018) 221–234.
[36] M. Carpentieri, A.G. Robins, P. Hayden, E. Santi, Mean and turbulent mass flux measurements in an idealised street network, Environ. Pollut. 234 (2018) 356–367.
[37] Y. Tominaga, Flow around a high-rise building using steady and unsteady RANS CFD: Effect of large-scale fluctuations on the velocity statistics, J. Wind Eng. Ind. Aerodyn. 142 (2015) 93–103.
[38] X. Cheng, Q. Zeng, F. Hu, Characteristics of gusty wind disturbances and turbulent fluctuations in windy atmospheric boundary layer behind cold fronts, J. Geophys. Res. Atmos. 116 (2011).
[39] K. Ahmad, M. Khare, K.K. Chaudhry, Wind tunnel simulation studies on dispersion at urban street canyons and intersections—a review, J. Wind Eng. Ind. Aerodyn. 93 (2005) 697–717.
[40] F.T. DePaul, C.M. Sheih, A tracer study of dispersion in an urban street canyon, Atmos. Environ. 19 (1985) 555–559. doi:https://doi.org/10.1016/0004-6981(85)90034-4.
[41] L.W. Chew, A.A. Aliabadi, L.K. Norford, Flows across high aspect ratio street canyons: Reynolds number independence revisited, Environ. Fluid Mech. 18 (2018) 1275–1291.
[42] P.-Y. Cui, Z. Li, W.-Q. Tao, Investigation of Re-independence of turbulent flow and pollutant dispersion in urban street canyon using numerical wind tunnel (NWT) models, Int. J. Heat Mass Transf. 79 (2014) 176–188.
[43] P.-Y. Cui, Z. Li, W.-Q. Tao, Numerical investigations on Re-independence for the turbulent flow and pollutant dispersion under the urban boundary layer with some experimental validations, Int. J. Heat Mass Transf. 106 (2017) 422–436.
[44] W. Kang, S.B. Lee, H.J. Sung, Self-sustained oscillations of turbulent flows over an open cavity, Exp. Fluids. 45 (2008) 693.
[45] Y. Nakamura, T.R. Oke, Wind, temperature and stability conditions in an east-west oriented urban canyon, Atmos. Environ.

22 (1988) 2691–2700.
[46] K. Nazridoust, G. Ahmadi, Airflow and pollutant transport in street canyons, J. Wind Eng. Ind. Aerodyn. 94 (2006) 491–522.
[47] R. Berkowicz, M. Ketzel, G. Vachon, P. Louka, J.-M. Rosant, P.G. Mestayer, J.-F. Sini, Examination of traffic pollution distribution in a street canyon using the Nantes' 99 experimental data and comparison with model results, Water, Air Soil Pollut. Focus. 2 (2002) 311–324.
[48] H. Huang, Y. Akutsu, M. Arai, M. Tamura, A two-dimensional air quality model in an urban street canyon: evaluation and sensitivity analysis, Atmos. Environ. 34 (2000) 689–698. doi:https://doi.org/10.1016/S1352-2310(99)00333-7.
[49] Y. Zhang, Z. Gu, Z. Wang, Y. Cheng, F.S.C. Lee, Advances in the fine scale simulation of urban wind environment, Indoor Built Environ. 22 (2013) 332–336.
[50] P. Louka, S.E. Belcher, R.G. Harrison, Coupling between air flow in streets and the well-developed boundary layer aloft, Atmos. Environ. 34 (2000) 2613–2621.
[51] W. Li, Y. He, Y. Zhang, Q. Shui, X. Wu, C.W. Yu, Z. Gu, Numerical study of the composite effects of uneven street canyons and time-varying inflows on the air flows and pollutant dispersion, Aerosol Air Qual. Res. 20 (2020) 1440–1453.
[52] S.M. Kwa, S.M. Salim, Numerical Simulation of Dispersion in an Urban Street Canyon: Comparison between Steady and Fluctuating Boundary Conditions., Eng. Lett. 23 (2015).
[53] F. Murena, B. Mele, Effect of short–time variations of wind velocity on mass transfer rate between street canyons and the atmospheric boundary layer, Atmos. Pollut. Res. 5 (2014) 484–490.
[54] A. Richter, B. Ruck, S. Mohr, M. Kunz, Interaction of severe convective gusts with a street canyon, Urban Clim. 23 (2018) 71–90.
[55] W.J. Li, Y. Zhang, B. Yang, J.W. Su, Y.W. Zhang, W.Z. Lu, Q.X. Shui, X.Y. Wu, Y.P. He, Z.L. Gu, Large-scale turbulence structures in a laboratory-scale boundary layer under steady and gusty wind inflows, Sci. Rep. 9 (2019) 1–15.
[56] G. Duan, K. Ngan, Effects of time-dependent inflow perturbations on turbulent flow in a street canyon, Boundary-Layer Meteorol. 167 (2018) 257–284.
[57] Y.-W. Zhang, Z.-L. Gu, Y. Cheng, S.-C. Lee, Effect of real-time boundary wind conditions on the air flow and pollutant dispersion in an urban street canyon—large eddy simulations, Atmos. Environ. 45 (2011) 3352–3359.
[58] W. Li, Y. He, Y. Zhang, J. Su, C. Chen, C.W. Yu, R. Zhang, Z. Gu, LES simulation of flow field and pollutant dispersion in a street canyon under time-varying inflows with TimeVarying-SIMPLE approach, Build. Environ. 157 (2019) 185–196.
[59] Y. Zhang, Z. Gu, C.W. Yu, Review on numerical simulation of airflow and pollutant dispersion in urban street canyons under natural background wind condition, Aerosol Air Qual. Res. 18 (2018) 780–789.
[60] Y. Zhang, Z. Gu, C.W. Yu, Impact Factors on Airflow and Pollutant Dispersion in Urban Street Canyons and Comprehensive Simulations: a Review, Curr. Pollut. Reports. (2020) 1–15.
[61] K. An, J.C.H. Fung, An improved SST k− ω model for pollutant dispersion simulations within an isothermal boundary layer, J. Wind Eng. Ind. Aerodyn. 179 (2018) 369–384.
[62] T. Okaze, A. Mochida, Cholesky decomposition–based generation of artificial inflow turbulence including scalar fluctuation, Comput. Fluids. 159 (2017) 23–32.
[63] Z.-T. Xie, I.P. Castro, Efficient generation of inflow conditions for large eddy simulation of street-scale flows, Flow, Turbul. Combust. 81 (2008) 449–470.
[64] Y. Liu, G. Cui, Z. Wang, W. Huang, C. Xu, Z. Zhang, A composite model for complex building street configuration in a large eddy simulation of local urban atmospheric environment, Sci. China Physics, Mech. Astron. 54 (2011) 716–723.
[65] X. Yang, F. Sotiropoulos, On the dispersion of contaminants released far upwind of a cubical building for different turbulent inflows, Build. Environ. 154 (2019) 324–335.
[66] S.H. Huang, Q.S. Li, J.R. Wu, A general inflow turbulence generator for large eddy simulation, J. Wind Eng. Ind. Aerodyn.

98 (2010) 600–617.
[67] J.-J. Kim, J.-J. Baik, Physical experiments to investigate the effects of street bottom heating and inflow turbulence on urban street-canyon flow, Adv. Atmos. Sci. 22 (2005) 230–237.
[68] R.F. Shi, G.X. Cui, Z.S. Wang, C.X. Xu, Z.S. Zhang, Large eddy simulation of wind field and plume dispersion in building array, Atmos. Environ. 42 (2008) 1083–1097.
[69] K. An, J.C.H. Fung, S.H.L. Yim, Sensitivity of inflow boundary conditions on downstream wind and turbulence profiles through building obstacles using a CFD approach, J. Wind Eng. Ind. Aerodyn. 115 (2013) 137–149. doi:https://doi.org/10.1016/j.jweia.2013.01.004.
[70] J.-J. Kim, J.-J. Baik, Effects of inflow turbulence intensity on flow and pollutant dispersion in an urban street canyon, J. Wind Eng. Ind. Aerodyn. 91 (2003) 309–329. doi:https://doi.org/10.1016/S0167-6105(02)00395-1.
[71] T. Michioka, A. Sato, H. Takimoto, M. Kanda, Large-Eddy Simulation for the Mechanism of Pollutant Removal from a Two-Dimensional Street Canyon, Boundary-Layer Meteorol. 138 (2011) 195–213. doi:10.1007/s10546-010-9556-2.
[72] T. Michioka, A. Sato, Effect of Incoming Turbulent Structure on Pollutant Removal from Two-Dimensional Street Canyon, Boundary-Layer Meteorol. 145 (2012) 469–484. doi:10.1007/s10546-012-9733-6.
[73] D.J. Wise, V.B.L. Boppana, K.W. Li, H.J. Poh, Effects of minor changes in the mean inlet wind direction on urban flow simulations, Sustain. Cities Soc. 37 (2018) 492–500. doi:https://doi.org/10.1016/j.scs.2017.11.041.
[74] L. Soulhac, R.J. Perkins, P. Salizzoni, Flow in a Street Canyon for any External Wind Direction, Boundary-Layer Meteorol. 126 (2008) 365–388. doi:10.1007/s10546-007-9238-x.
[75] S. Vardoulakis, B.E.A. Fisher, K. Pericleous, N. Gonzalez-Flesca, Modelling air quality in street canyons: a review, Atmos. Environ. 37 (2003) 155–182. doi:https://doi.org/10.1016/S1352-2310(02)00857-9.
[76] P.S.J. Buller, Wind speeds measured within an urban area, in: Rep. No. 2, Department of Environment Building Research Station, Watford, UK, 1976.
[77] M. Schatzmann, B. Leitl, Issues with validation of urban flow and dispersion CFD models, J. Wind Eng. Ind. Aerodyn. 99 (2011) 169–186. doi:https://doi.org/10.1016/j.jweia.2011.01.005.
[78] P. Kastner-Klein, E.J. Plate, Wind-tunnel study of concentration fields in street canyons, Atmos. Environ. 33 (1999) 3973–3979. doi:https://doi.org/10.1016/S1352-2310(99)00139-9.
[79] L. Soulhac, P. Salizzoni, Dispersion in a street canyon for a wind direction parallel to the street axis, J. Wind Eng. Ind. Aerodyn. 98 (2010) 903–910. doi:https://doi.org/10.1016/j.jweia.2010.09.004.
[80] K. Blackman, L. Perret, E. Savory, T. Piquet, Field and wind tunnel modeling of an idealized street canyon flow, Atmos. Environ. 106 (2015) 139–153. doi:https://doi.org/10.1016/j.atmosenv.2015.01.067.
[81] J.-J. Kim, J.-J. Baik, A numerical study of the effects of ambient wind direction on flow and dispersion in urban street canyons using the RNG k–ε turbulence model, Atmos. Environ. 38 (2004) 3039–3048. doi:https://doi.org/10.1016/j.atmosenv.2004.02.047.
[82] M. Lin, J. Hang, Y. Li, Z. Luo, M. Sandberg, Quantitative ventilation assessments of idealized urban canopy layers with various urban layouts and the same building packing density, Build. Environ. 79 (2014) 152–167. doi:https://doi.org/10.1016/j.buildenv.2014.05.008.
[83] R. Ramponi, B. Blocken, L.B. de Coo, W.D. Janssen, CFD simulation of outdoor ventilation of generic urban configurations with different urban densities and equal and unequal street widths, Build. Environ. 92 (2015) 152–166. doi:https://doi.org/10.1016/j.buildenv.2015.04.018.
[84] D.M.S. Madalozzo, A.L. Braun, A.M. Awruch, I.B. Morsch, Numerical simulation of pollutant dispersion in street canyons: geometric and thermal effects, Appl. Math. Model. 38 (2014) 5883–5909.
[85] L. Huizhi, L. Bin, Z. Fengrong, Z. Boyin, S. Jianguo, A laboratory model for the flow in urban street canyons induced by bottom heating, Adv. Atmos. Sci. 20 (2003) 554.

[86] A.S. Adelia, C. Yuan, L. Liu, R.Q. Shan, Effects of urban morphology on anthropogenic heat dispersion in tropical high-density residential areas, Energy Build. 186 (2019) 368–383.
[87] G. Duan, K. Ngan, Sensitivity of turbulent flow around a 3-D building array to urban boundary-layer stability, J. Wind Eng. Ind. Aerodyn. 193 (2019) 103958. doi:https://doi.org/10.1016/j.jweia.2019.103958.
[88] P. Louka, G. Vachon, J.-F. Sini, P.G. Mestayer, J.-M. Rosant, Thermal effects on the airflow in a street canyon–Nantes' 99 experimental results and model simulations, Water, Air Soil Pollut. Focus. 2 (2002) 351–364.
[89] X.-X. Li, R. Britter, L.K. Norford, Effect of stable stratification on dispersion within urban street canyons: A large-eddy simulation, Atmos. Environ. 144 (2016) 47–59.
[90] K. Uehara, S. Murakami, S. Oikawa, S. Wakamatsu, Wind tunnel experiments on how thermal stratification affects flow in and above urban street canyons, Atmos. Environ. 34 (2000) 1553–1562. doi:https://doi.org/10.1016/S1352-2310(99)00410-0.
[91] A. Simón-Moral, J.L. Santiago, A. Martilli, Effects of unstable thermal stratification on vertical fluxes of heat and momentum in urban areas, Boundary-Layer Meteorol. 163 (2017) 103–121.
[92] J.M. Tomas, M. Pourquie, H.J.J. Jonker, Stable stratification effects on flow and pollutant dispersion in boundary layers entering a generic urban environment, Boundary-Layer Meteorol. 159 (2016) 221–239.
[93] V.B.L. Boppana, Z.-T. Xie, I.P. Castro, Thermal stratification effects on flow over a generic urban canopy, Boundary-Layer Meteorol. 153 (2014) 141–162.
[94] X.-X. Li, C.-H. Liu, D.Y.C. Leung, Parallel FEM LES with one-equation subgrid-scale model for incompressible flows, Int. J. Comut. Fluid Dyn. 24 (2010) 37–49.
[95] W.C. Cheng, C.-H. Liu, Large-eddy simulation of turbulent transports in urban street canyons in different thermal stabilities, J. Wind Eng. Ind. Aerodyn. 99 (2011) 434–442.
[96] Z. Shen, G. Cui, Z. Zhang, Turbulent dispersion of pollutants in urban-type canopies under stable stratification conditions, Atmos. Environ. 156 (2017) 1–14.
[97] X.-X. Li, R.E. Britter, L.K. Norford, T.-Y. Koh, D. Entekhabi, Flow and pollutant transport in urban street canyons of different aspect ratios with ground heating: large-eddy simulation, Boundary-Layer Meteorol. 142 (2012) 289–304.
[98] X.-X. Li, R.E. Britter, T.Y. Koh, L.K. Norford, C.-H. Liu, D. Entekhabi, D.Y.C. Leung, Large-eddy simulation of flow and pollutant transport in urban street canyons with ground heating, Boundary-Layer Meteorol. 137 (2010) 187–204.
[99] W.C. Cheng, C.-H. Liu, D.Y.C. Leung, On the correlation of air and pollutant exchange for street canyons in combined wind-buoyancy-driven flow, Atmos. Environ. 43 (2009) 3682–3690.
[100] S.-B. Park, J.-J. Baik, S. Raasch, M.O. Letzel, A large-eddy simulation study of thermal effects on turbulent flow and dispersion in and above a street canyon, J. Appl. Meteorol. Climatol. 51 (2012) 829–841.
[101] G. Jiang, T. Hu, H. Yang, Effects of Ground Heating on Ventilation and Pollutant Transport in Three-Dimensional Urban Street Canyons with Unit Aspect Ratio, Atmosphere (Basel). 10 (2019) 286.
[102] P.J.C. Schrijvers, H.J.J. Jonker, S.R. de Roode, S. Kenjereš, On the daytime micro-climatic conditions inside an idealized 2D urban canyon, Build. Environ. 167 (2020) 106427. doi:https://doi.org/10.1016/j.buildenv.2019.106427.
[103] J.L. Santiago, E.S. Krayenhoff, A. Martilli, Flow simulations for simplified urban configurations with microscale distributions of surface thermal forcing, Urban Clim. 9 (2014) 115–133. doi:https://doi.org/10.1016/j.uclim.2014.07.008.
[104] X. Xie, C.-H. Liu, D.Y.C. Leung, Impact of building facades and ground heating on wind flow and pollutant transport in street canyons, Atmos. Environ. 41 (2007) 9030–9049. doi:https://doi.org/10.1016/j.atmosenv.2007.08.027.
[105] W. Liang, J. Huang, P. Jones, Q. Wang, J. Hang, A zonal model for assessing street canyon air temperature of high-density cities, Build. Environ. 132 (2018) 160–169.
[106] J. Hang, X. Chen, G. Chen, T. Chen, Y. Lin, Z. Luo, X. Zhang, Q. Wang, The influence of aspect ratios and wall heating conditions on flow and passive pollutant exposure in 2D typical street canyons, Build. Environ. (2019) 106536. doi:https://doi.org/10.1016/j.buildenv.2019.106536.

[107] X.-M. Cai, Effects of Wall Heating on Flow Characteristics in a Street Canyon, Boundary-Layer Meteorol. 142 (2012) 443–467. doi:10.1007/s10546-011-9681-6.
[108] X. Cai, Effects of differential wall heating in street canyons on dispersion and ventilation characteristics of a passive scalar, Atmos. Environ. 51 (2012) 268–277. doi:https://doi.org/10.1016/j.atmosenv.2012.01.010.
[109] J. Allegrini, V. Dorer, J. Carmeliet, Wind tunnel measurements of buoyant flows in street canyons, Build. Environ. 59 (2013) 315–326. doi:https://doi.org/10.1016/j.buildenv.2012.08.029.
[110] J.-J. Kim, J.-J. Baik, A numerical study of thermal effects on flow and pollutant dispersion in urban street canyons, J. Appl. Meteorol. 38 (1999) 1249–1261.
[111] Y. Lin, T. Ichinose, Y. Yamao, H. Mouri, Wind velocity and temperature fields under different surface heating conditions in a street canyon in wind tunnel experiments, Build. Environ. 168 (2020) 106500. doi:https://doi.org/10.1016/j.buildenv.2019.106500.
[112] L.W. Chew, L.R. Glicksman, L.K. Norford, Buoyant flows in street canyons: Comparison of RANS and LES at reduced and full scales, Build. Environ. 146 (2018) 77–87.
[113] Z. Li, H. Zhang, C.-Y. Wen, A.-S. Yang, Y.-H. Juan, Effects of frontal area density on outdoor thermal comfort and air quality, Build. Environ. 180 (2020) 107028. doi:https://doi.org/10.1016/j.buildenv.2020.107028.
[114] Z. Li, H. Zhang, C.-Y. Wen, A.-S. Yang, Y.-H. Juan, Effects of height-asymmetric street canyon configurations on outdoor air temperature and air quality, Build. Environ. (2020) 107195.
[115] Z. Tan, J. Dong, Y. Xiao, J. Tu, A numerical study of diurnally varying surface temperature on flow patterns and pollutant dispersion in street canyons, Atmos. Environ. 104 (2015) 217–227. doi:https://doi.org/10.1016/j.atmosenv.2015.01.027.
[116] S. Bottillo, A.D.L. Vollaro, G. Galli, A. Vallati, Fluid dynamic and heat transfer parameters in an urban canyon, Sol. Energy. 99 (2014) 1–10. doi:https://doi.org/10.1016/j.solener.2013.10.031.
[117] S. Bottillo, A.D.L. Vollaro, G. Galli, A. Vallati, CFD modeling of the impact of solar radiation in a tridimensional urban canyon at different wind conditions, Sol. Energy. 102 (2014) 212–222. doi:https://doi.org/10.1016/j.solener.2014.01.029.
[118] Y. Qu, M. Milliez, L. Musson-Genon, B. Carissimo, Numerical study of the thermal effects of buildings on low-speed airflow taking into account 3D atmospheric radiation in urban canopy, J. Wind Eng. Ind. Aerodyn. 104–106 (2012) 474–483. doi:https://doi.org/10.1016/j.jweia.2012.03.008.
[119] N. Nazarian, A. Martilli, J. Kleissl, Impacts of realistic urban heating, part I: spatial variability of mean flow, turbulent exchange and pollutant dispersion, Boundary-Layer Meteorol. 166 (2018) 367–393.
[120] N. Nazarian, A. Martilli, L. Norford, J. Kleissl, Impacts of realistic urban heating. Part II: air quality and city breathability, Boundary-Layer Meteorol. 168 (2018) 321–341.
[121] N. Nazarian, J. Kleissl, Realistic solar heating in urban areas: Air exchange and street-canyon ventilation, Build. Environ. 95 (2016) 75–93. doi:https://doi.org/10.1016/j.buildenv.2015.08.021.
[122] Y. Qin, S.C. Kot, Dispersion of vehicular emission in street canyons, Guangzhou City, South China (P.R.C.), Atmos. Environ. Part B. Urban Atmos. 27 (1993) 283–291. doi:https://doi.org/10.1016/0957-1272(93)90023-Y.
[123] Z. Li, J. Xu, T. Ming, C. Peng, J. Huang, T. Gong, Numerical simulation on the effect of vehicle movement on pollutant dispersion in urban street, Procedia Eng. 205 (2017) 2303–2310.
[124] N.A. Mazzeo, L.E. Venegas, 5.22 EVALUATION OF TURBULENCE FROM TRAFFIC USING EXPERIMENTAL DATA OBTAINED IN A STREET CANYON, (2005).
[125] A.M. Sahlodin, R. Sotudeh-Gharebagh, Y. Zhu, Modeling of dispersion near roadways based on the vehicle-induced turbulence concept, Atmos. Environ. 41 (2007) 92–102.
[126] J. Pospisil, M. Jicha, Particulate matter dispersion modelling along urban traffic paths, Int. J. Environ. Pollut. 40 (2010) 26–35.
[127] M. Jicha, J. Pospisil, J. Katolicky, Dispersion of pollutants in street canyon under traffic induced flow and turbulence,

Environ. Monit. Assess. 65 (2000) 343–351.
[128] Y.-W. Zhang, Z.-L. Gu, Y. Cheng, Z.-X. Shen, J.-G. Dong, S.-C. Lee, Measurement of diurnal variations of PM2. 5 mass concentrations and factors affecting pollutant dispersion in urban street canyons under weak-wind conditions in Xi'an, Aerosol Air Qual. Res. 12 (2012) 1261–1268.
[129] T. Shi, T. Ming, Y. Wu, C. Peng, Y. Fang, R. de_Richter, The effect of exhaust emissions from a group of moving vehicles on pollutant dispersion in the street canyons, Build. Environ. 181 (2020) 107120. doi:https://doi.org/10.1016/j.buildenv.2020.107120.
[130] N. Kalthoff, D. Bäumer, U. Corsmeier, M. Kohler, B. Vogel, Vehicle-induced turbulence near a motorway, Atmos. Environ. 39 (2005) 5737–5749. doi:https://doi.org/10.1016/j.atmosenv.2004.06.048.
[131] P. Kastner-Klein, R. Berkowicz, E.J. Plate, Modelling of vehicle-induced turbulence in air pollution studies for streets, Int. J. Environ. Pollut. 14 (2000) 496–507.
[132] A. Alonso-Estébanez, P. Pascual-Muñoz, C. Yagüe, R. Laina, D. Castro-Fresno, Field experimental study of traffic-induced turbulence on highways, Atmos. Environ. 61 (2012) 189–196.
[133] H. Kondo, T. Tomizuka, A numerical experiment of roadside diffusion under traffic-produced flow and turbulence, Atmos. Environ. 43 (2009) 4137–4147.
[134] L. Sedefian, S. Trivikrama Rao, U. Czapski, Effects of traffic-generated turbulence on near-field dispersion, Atmos. Environ. 15 (1981) 527–536. doi:https://doi.org/10.1016/0004-6981(81)90182-7.
[135] H. Woodward, M. Stettler, D. Pavlidis, E. Aristodemou, H. ApSimon, C. Pain, A large eddy simulation of the dispersion of traffic emissions by moving vehicles at an intersection, Atmos. Environ. 215 (2019) 116891.
[136] S. Di Sabatino, P. Kastner-Klein, R. Berkowicz, R.E. Britter, E. Fedorovich, The modelling of turbulence from traffic in urban dispersion models—Part I: theoretical considerations, Environ. Fluid Mech. 3 (2003) 129–143.
[137] Q. Wang, W. Fang, R. de Richter, C. Peng, T. Ming, Effect of moving vehicles on pollutant dispersion in street canyon by using dynamic mesh updating method, J. Wind Eng. Ind. Aerodyn. 187 (2019) 15–25.
[138] M. He, S. Dhaniyala, A dispersion model for traffic produced turbulence in a two-way traffic scenario, Environ. Fluid Mech. 11 (2011) 627–640.
[139] J. Pospisil, M. Jicha, Influence of vehicle-induced turbulence on pollutant dispersion in street canyon and adjacent urban area, Int. J. Environ. Pollut. 62 (2017) 89–101.
[140] C. Cai, T. Ming, W. Fang, R. de Richter, C. Peng, The effect of turbulence induced by different kinds of moving vehicles in street canyons, Sustain. Cities Soc. 54 (2020) 102015. doi:https://doi.org/10.1016/j.scs.2020.102015.
[141] B. Offerle, I. Eliasson, C.S.B. Grimmond, B. Holmer, Surface heating in relation to air temperature, wind and turbulence in an urban street canyon, Boundary-Layer Meteorol. 122 (2007) 273–292. doi:10.1007/s10546-006-9099-8.
[142] I. Kanda, Y. Yamao, Passive scalar diffusion in and above urban-like roughness under weakly stable and unstable thermal stratification conditions, J. Wind Eng. Ind. Aerodyn. 148 (2016) 18–33. doi:https://doi.org/10.1016/j.jweia.2015.11.002.
[143] J. Hang, X. Chen, G. Chen, T. Chen, Y. Lin, Z. Luo, X. Zhang, Q. Wang, The influence of aspect ratios and wall heating conditions on flow and passive pollutant exposure in 2D typical street canyons, Build. Environ. 168 (2020) 106536. doi:https://doi.org/10.1016/j.buildenv.2019.106536.
[144] X. Xie, C.-H. Liu, D.Y.C. Leung, M.K.H. Leung, Characteristics of air exchange in a street canyon with ground heating, Atmos. Environ. 40 (2006) 6396–6409. doi:https://doi.org/10.1016/j.atmosenv.2006.05.050.
[145] E. Solazzo, S. Vardoulakis, X. Cai, Evaluation of traffic-producing turbulence schemes within operational street pollution models using roadside measurements, Atmos. Environ. 41 (2007) 5357–5370.
[146] Y. Zhang, Z. Gu, C.W. Yu, Large eddy simulation of vehicle induced turbulence in an urban street canyon with a new dynamically vehicle-tracking scheme, Aerosol Air Qual. Res. 17 (2017) 865–874.
[147] A. Rastetter, Experimentelle Untersuchung in einem atmosphärischen Grenzschichtwindkanal über den Einfluß von Kfz-

erzeugter Turbulenz auf die Schadstoffausbreitung in Straßenschluchten, (1997).
[148] F. Yang, F. Qian, S.S.Y. Lau, Urban form and density as indicators for summertime outdoor ventilation potential: A case study on high-rise housing in Shanghai, Build. Environ. 70 (2013) 122–137. doi:https://doi.org/10.1016/j.buildenv.2013.08.019.
[149] A.-S. Yang, Y.-H. Juan, C.-Y. Wen, Y.-M. Su, Y.-C. Wu, Investigation on wind environments of surrounding open spaces around a public building, J. Mech. 33 (2017) 101–113.
[150] A.-S. Yang, C.-Y. Wen, Y.-H. Juan, Y.-M. Su, J.-H. Wu, Using the central ventilation shaft design within public buildings for natural aeration enhancement, Appl. Therm. Eng. 70 (2014) 219–230. doi:https://doi.org/10.1016/j.applthermaleng.2014.05.017.
[151] P. Gousseau, B. Blocken, T. Stathopoulos, G.J.F. Van Heijst, CFD simulation of near-field pollutant dispersion on a high-resolution grid: a case study by LES and RANS for a building group in downtown Montreal, Atmos. Environ. 45 (2011) 428–438.
[152] B.-J. He, L. Ding, D. Prasad, Relationships among local-scale urban morphology, urban ventilation, urban heat island and outdoor thermal comfort under sea breeze influence, Sustain. Cities Soc. (2020) 102289.
[153] B.-J. He, Potentials of meteorological characteristics and synoptic conditions to mitigate urban heat island effects, Urban Clim. 24 (2018) 26–33.
[154] P. Edussuriya, A. Chan, A. Ye, Urban morphology and air quality in dense residential environments in Hong Kong. Part I: District-level analysis, Atmos. Environ. 45 (2011) 4789–4803. doi:https://doi.org/10.1016/j.atmosenv.2009.07.061.
[155] H. Dou, T. Ming, Z. Li, C. Peng, C. Zhang, X. Fu, Numerical simulation of pollutant dispersion characteristics in a three-dimensional urban traffic system, Atmos. Pollut. Res. 9 (2018) 735–746.
[156] T. Ming, W. Fang, C. Peng, C. Cai, R. De Richter, M.H. Ahmadi, Y. Wen, Impacts of traffic tidal flow on pollutant dispersion in a non-uniform urban street canyon, Atmosphere (Basel). 9 (2018) 82.
[157] C. Yuan, E. Ng, L.K. Norford, Improving air quality in high-density cities by understanding the relationship between air pollutant dispersion and urban morphologies, Build. Environ. 71 (2014) 245–258.
[158] L.W. Chew, L.K. Norford, Pedestrian-level wind speed enhancement in urban street canyons with void decks, Build. Environ. 146 (2018) 64–76. doi:https://doi.org/10.1016/j.buildenv.2018.09.039.
[159] J. Zhang, L. Xu, V. Shabunko, S.E.R. Tay, H. Sun, S.S.Y. Lau, T. Reindl, Impact of urban block typology on building solar potential and energy use efficiency in tropical high-density city, Appl. Energy. 240 (2019) 513–533. doi:https://doi.org/10.1016/j.apenergy.2019.02.033.
[160] R.E. Britter, S.R. Hanna, Flow and dispersion in urban areas, Annu. Rev. Fluid Mech. 35 (2003) 469–496.
[161] P.-Y. Cui, Z. Li, W.-Q. Tao, Wind-tunnel measurements for thermal effects on the air flow and pollutant dispersion through different scale urban areas, Build. Environ. 97 (2016) 137–151.
[162] Y. Gao, Z. Wang, C. Liu, Z.-R. Peng, Assessing neighborhood air pollution exposure and its relationship with the urban form, Build. Environ. 155 (2019) 15–24.
[163] S. Wu, F. Deng, J. Niu, Q. Huang, Y. Liu, X. Guo, Association of heart rate variability in taxi drivers with marked changes in particulate air pollution in Beijing in 2008, Environ. Health Perspect. 118 (2010) 87–91.
[164] J. Yang, X. Fu, The Centre of City: Wind Environment and Spatial Morphology, Springer, 2019.
[165] M. Hadavi, H. Pasdarshahri, Quantifying impacts of wind speed and urban neighborhood layout on the infiltration rate of residential buildings, Sustain. Cities Soc. 53 (2020) 101887. doi:https://doi.org/10.1016/j.scs.2019.101887.
[166] Y. Xu, C. Ren, P. Ma, J. Ho, W. Wang, K.K.-L. Lau, H. Lin, E. Ng, Urban morphology detection and computation for urban climate research, Landsc. Urban Plan. 167 (2017) 212–224. doi:https://doi.org/10.1016/j.landurbplan.2017.06.018.
[167] T. Kubota, M. Miura, Y. Tominaga, A. Mochida, Wind tunnel tests on the relationship between building density and pedestrian-level wind velocity: Development of guidelines for realizing acceptable wind environment in residential neighborhoods, Build. Environ. 43 (2008) 1699–1708. doi:https://doi.org/10.1016/j.buildenv.2007.10.015.

[168] R. Buccolieri, M. Sandberg, S. Di Sabatino, City breathability and its link to pollutant concentration distribution within urban-like geometries, Atmos. Environ. 44 (2010) 1894–1903. doi:https://doi.org/10.1016/j.atmosenv.2010.02.022.
[169] J. Yang, B. Shi, Y. Zheng, Y. Shi, G. Xia, Urban form and air pollution disperse: Key indexes and mitigation strategies, Sustain. Cities Soc. 57 (2020) 101955. doi:https://doi.org/10.1016/j.scs.2019.101955.
[170] K. Hu, S. Cheng, Y. Qian, CFD Simulation Analysis of Building Density on Residential Wind Environment., J. Eng. Sci. Technol. Rev. 11 (2018).
[171] S. Di Sabatino, R. Buccolieri, B. Pulvirenti, R. Britter, Simulations of pollutant dispersion within idealised urban-type geometries with CFD and integral models, Atmos. Environ. 41 (2007) 8316–8329. doi:https://doi.org/10.1016/j.atmosenv.2007.06.052.
[172] J. Srebric, M. Heidarinejad, J. Liu, Building neighborhood emerging properties and their impacts on multi-scale modeling of building energy and airflows, Build. Environ. 91 (2015) 246–262. doi:https://doi.org/10.1016/j.buildenv.2015.02.031.
[173] S.H.L. Yim, J.C.H. Fung, A.K.H. Lau, S.C. Kot, Air ventilation impacts of the “wall effect” resulting from the alignment of high-rise buildings, Atmos. Environ. 43 (2009) 4982–4994. doi:https://doi.org/10.1016/j.atmosenv.2009.07.002.
[174] M. Carpentieri, A.G. Robins, Influence of urban morphology on air flow over building arrays, J. Wind Eng. Ind. Aerodyn. 145 (2015) 61–74. doi:https://doi.org/10.1016/j.jweia.2015.06.001.
[175] L. Li, X. Yang, Y. Qian, CFD Simulation Analysis of the Influence of Floor Area Ratio on the Wind Environment in Residential Districts., J. Eng. Sci. Technol. Rev. 11 (2018) 185–192.
[176] T. Bentham, R. Britter, Spatially averaged flow within obstacle arrays, Atmos. Environ. 37 (2003) 2037–2043. doi:https://doi.org/10.1016/S1352-2310(03)00123-7.
[177] S.-J. Mei, J.-T. Hu, D. Liu, F.-Y. Zhao, Y. Li, Y. Wang, H.-Q. Wang, Wind driven natural ventilation in the idealized building block arrays with multiple urban morphologies and unique package building density, Energy Build. 155 (2017) 324–338. doi:https://doi.org/10.1016/j.enbuild.2017.09.019.
[178] Y. Shi, K.K.-L. Lau, E. Ng, Incorporating wind availability into land use regression modelling of air quality in mountainous high-density urban environment, Environ. Res. 157 (2017) 17–29. doi:https://doi.org/10.1016/j.envres.2017.05.007.
[179] E. Ng, C. Yuan, L. Chen, C. Ren, J.C.H. Fung, Improving the wind environment in high-density cities by understanding urban morphology and surface roughness: A study in Hong Kong, Landsc. Urban Plan. 101 (2011) 59–74. doi:https://doi.org/10.1016/j.landurbplan.2011.01.004.
[180] A. Abd Razak, A. Hagishima, N. Ikegaya, J. Tanimoto, Analysis of airflow over building arrays for assessment of urban wind environment, Build. Environ. 59 (2013) 56–65. doi:https://doi.org/10.1016/j.buildenv.2012.08.007.
[181] M. Bady, S. Kato, H. Huang, Towards the application of indoor ventilation efficiency indices to evaluate the air quality of urban areas, Build. Environ. 43 (2008) 1991–2004. doi:https://doi.org/10.1016/j.buildenv.2007.11.013.
[182] M. Shirzadi, M. Naghashzadegan, P. A. Mirzaei, Improving the CFD modelling of cross-ventilation in highly-packed urban areas, Sustain. Cities Soc. 37 (2018) 451–465. doi:https://doi.org/10.1016/j.scs.2017.11.020.
[183] J.O.P. Cheung, C.-H. Liu, CFD simulations of natural ventilation behaviour in high-rise buildings in regular and staggered arrangements at various spacings, Energy Build. 43 (2011) 1149–1158. doi:https://doi.org/10.1016/j.enbuild.2010.11.024.
[184] M.N.A.W.M. Yazid, A.S.B. Sharif, N.A. Che, M.H.H. Sidik, F.M. Zawawi, U. Abidin, Effects of Staggered Array of Cubical Obstacles on Near-Ground Wind Environment and Air Quality, J. Adv. Res. Fluid Mech. Therm. Sci. 58 (2019) 261–274.
[185] H. Cheng, I.P. Castro, Near Wall Flow over Urban-like Roughness, Boundary-Layer Meteorol. 104 (2002) 229–259. doi:10.1023/A:1016060103448.
[186] J. Hang, Y. Li, Ventilation strategy and air change rates in idealized high-rise compact urban areas, Build. Environ. 45 (2010) 2754–2767. doi:https://doi.org/10.1016/j.buildenv.2010.06.004.
[187] N. Antoniou, H. Montazeri, H. Wigo, M.K.-A. Neophytou, B. Blocken, M. Sandberg, CFD and wind-tunnel analysis of

outdoor ventilation in a real compact heterogeneous urban area: Evaluation using “air delay,” Build. Environ. 126 (2017) 355–372. doi:https://doi.org/10.1016/j.buildenv.2017.10.013.

[188] J. Hang, Y. Li, M. Sandberg, Experimental and numerical studies of flows through and within high-rise building arrays and their link to ventilation strategy, J. Wind Eng. Ind. Aerodyn. 99 (2011) 1036–1055. doi:https://doi.org/10.1016/j.jweia.2011.07.004.

[189] Y. Ishida, T. Okaze, A. Mochida, Influence of urban configuration on the structure of kinetic energy transport and the energy dissipation rate, J. Wind Eng. Ind. Aerodyn. 183 (2018) 198–213. doi:https://doi.org/10.1016/j.jweia.2018.10.016.

[190] L. Chen, J. Hang, M. Sandberg, L. Claesson, S. Di Sabatino, H. Wigo, The impacts of building height variations and building packing densities on flow adjustment and city breathability in idealized urban models, Build. Environ. 118 (2017) 344–361. doi:https://doi.org/10.1016/j.buildenv.2017.03.042.

[191] W. Wang, E. Ng, C. Yuan, S. Raasch, Large-eddy simulations of ventilation for thermal comfort — A parametric study of generic urban configurations with perpendicular approaching winds, Urban Clim. 20 (2017) 202–227. doi:https://doi.org/10.1016/j.uclim.2017.04.007.

[192] W. Wang, E. Ng, Large-eddy simulations of air ventilation in parametric scenarios: comparative studies of urban form and wind direction, Archit. Sci. Rev. 61 (2018) 215–225.

[193] D.J. Cui, C.M. Mak, Z.T. Ai, K.C.S. Kwok, X.Z. Meng, J.L. Niu, On-site evaluation of pedestrian-level air quality at a U-type street canyon in an ancient city, J. Wind Eng. Ind. Aerodyn. 168 (2017) 322–333. doi:https://doi.org/10.1016/j.jweia.2017.06.014.

[194] Q.M. Zahid Iqbal, A.L.S. Chan, Pedestrian level wind environment assessment around group of high-rise cross-shaped buildings: Effect of building shape, separation and orientation, Build. Environ. 101 (2016) 45–63. doi:https://doi.org/10.1016/j.buildenv.2016.02.015.

[195] D. Cui, G. Hu, Z. Ai, Y. Du, C.M. Mak, K. Kwok, Particle image velocimetry measurement and CFD simulation of pedestrian level wind environment around U-type street canyon, Build. Environ. 154 (2019) 239–251. doi:https://doi.org/10.1016/j.buildenv.2019.03.025.

[196] W.C. Cheng, C.-H. Liu, Large-Eddy Simulation of Flow and Pollutant Transports in and Above Two-Dimensional Idealized Street Canyons, Boundary-Layer Meteorol. 139 (2011) 411–437. doi:10.1007/s10546-010-9584-y.

[197] T.R. Oke, Street design and urban canopy layer climate, Energy Build. 11 (1988) 103–113.

[198] X. Xiaomin, H. Zhen, W. Jiasong, The impact of urban street layout on local atmospheric environment, Build. Environ. 41 (2006) 1352–1363.

[199] C.-Y. Wen, Y.-H. Juan, A.-S. Yang, Enhancement of city breathability with half open spaces in ideal urban street canyons, Build. Environ. 112 (2017) 322–336. doi:https://doi.org/10.1016/j.buildenv.2016.11.048.

[200] Z. Li, T. Shi, Y. Wu, H. Zhang, Y.-H. Juan, T. Ming, N. Zhou, Effect of traffic tidal flow on pollutant dispersion in various street canyons and corresponding mitigation strategies, Energy Built Environ. 1 (2020) 242–253. doi:https://doi.org/10.1016/j.enbenv.2020.02.002.

[201] K. Zhang, G. Chen, Y. Zhang, S. Liu, X. Wang, B. Wang, J. Hang, Integrated impacts of turbulent mixing and NOX-O3 photochemistry on reactive pollutant dispersion and intake fraction in shallow and deep street canyons, Sci. Total Environ. 712 (2020) 135553. doi:https://doi.org/10.1016/j.scitotenv.2019.135553.

[202] K. Zhang, G. Chen, X. Wang, S. Liu, C.M. Mak, Y. Fan, J. Hang, Numerical evaluations of urban design technique to reduce vehicular personal intake fraction in deep street canyons, Sci. Total Environ. 653 (2019) 968–994. doi:https://doi.org/10.1016/j.scitotenv.2018.10.333.

[203] C.-H. Liu, W.C. Cheng, T.C.Y. Leung, D.Y.C. Leung, On the mechanism of air pollutant re-entrainment in two-dimensional idealized street canyons, Atmos. Environ. 45 (2011) 4763–4769. doi:https://doi.org/10.1016/j.atmosenv.2010.03.015.

[204] C. Yuan, E. Ng, Building porosity for better urban ventilation in high-density cities – A computational parametric study, Build. Environ. 50 (2012) 176–189. doi:https://doi.org/10.1016/j.buildenv.2011.10.023.
[205] Y. Du, C.M. Mak, Improving pedestrian level low wind velocity environment in high-density cities: A general framework and case study, Sustain. Cities Soc. 42 (2018) 314–324. doi:https://doi.org/10.1016/j.scs.2018.08.001.
[206] K. An, S.-M. Wong, J.C.-H. Fung, Exploration of sustainable building morphologies for effective passive pollutant dispersion within compact urban environments, Build. Environ. 148 (2019) 508–523. doi:https://doi.org/10.1016/j.buildenv.2018.11.030.
[207] F. Yang, Y. Gao, K. Zhong, Y. Kang, Impacts of cross-ventilation on the air quality in street canyons with different building arrangements, Build. Environ. 104 (2016) 1–12. doi:https://doi.org/10.1016/j.buildenv.2016.04.013.
[208] HKBD (Hong Kong Buildings Department), Practice notes for authorized persons, registered structural engineers and registered geotechnical engineers, no. APP-152 — sustainable building design guidelines, (2011).
[209] W.-Y. Ng, C.-K. Chau, A modeling investigation of the impact of street and building configurations on personal air pollutant exposure in isolated deep urban canyons, Sci. Total Environ. 468–469 (2014) 429–448. doi:https://doi.org/10.1016/j.scitotenv.2013.08.077.
[210] M. Fan, C.K. Chau, E.H.W. Chan, J. Jia, A decision support tool for evaluating the air quality and wind comfort induced by different opening configurations for buildings in canyons, Sci. Total Environ. 574 (2017) 569–582. doi:https://doi.org/10.1016/j.scitotenv.2016.09.083.
[211] J. Shen, Z. Gao, W. Ding, Y. Yu, An investigation on the effect of street morphology to ambient air quality using six real-world cases, Atmos. Environ. 164 (2017) 85–101. doi:https://doi.org/10.1016/j.atmosenv.2017.05.047.
[212] C. Hao, X. Xie, Y. Huang, Z. Huang, Study on influence of viaduct and noise barriers on the particulate matter dispersion in street canyons by CFD modeling, Atmos. Pollut. Res. 10 (2019) 1723–1735.
[213] J. Hang, M. Lin, D.C. Wong, X. Wang, B. Wang, R. Buccolieri, On the influence of viaduct and ground heating on pollutant dispersion in 2D street canyons and toward single-sided ventilated buildings, Atmos. Pollut. Res. 7 (2016) 817–832. doi:https://doi.org/10.1016/j.apr.2016.04.009.
[214] H. Zhi, Z. Qiu, W. Wang, G. Wang, Y. Hao, Y. Liu, The influence of a viaduct on PM dispersion in a typical street: Field experiment and numerical simulations, Atmos. Pollut. Res. 11 (2020) 815–824. doi:https://doi.org/10.1016/j.apr.2020.01.009.
[215] G. Duan, P. Brimblecombe, Y.L. Chu, K. Ngan, Turbulent flow and dispersion inside and around elevated walkways, Build. Environ. 173 (2020) 106711. doi:https://doi.org/10.1016/j.buildenv.2020.106711.
[216] Y. Huang, Z. Zhou, A Numerical Study of Airflow and Pollutant Dispersion Inside an Urban Street Canyon Containing an Elevated Expressway, Environ. Model. Assess. 18 (2013) 105–114. doi:10.1007/s10666-012-9332-4.
[217] S. Ding, Y. Huang, P. Cui, J. Wu, M. Li, D. Liu, Impact of viaduct on flow reversion and pollutant dispersion in 2D urban street canyon with different roof shapes - Numerical simulation and wind tunnel experiment, Sci. Total Environ. 671 (2019) 976–991. doi:https://doi.org/10.1016/j.scitotenv.2019.03.391.
[218] J. Hang, Z. Luo, X. Wang, L. He, B. Wang, W. Zhu, The influence of street layouts and viaduct settings on daily carbon monoxide exposure and intake fraction in idealized urban canyons, Environ. Pollut. 220 (2017) 72–86. doi:https://doi.org/10.1016/j.envpol.2016.09.024.
[219] L. He, J. Hang, X. Wang, B. Lin, X. Li, G. Lan, Numerical investigations of flow and passive pollutant exposure in high-rise deep street canyons with various street aspect ratios and viaduct settings, Sci. Total Environ. 584–585 (2017) 189–206. doi:https://doi.org/10.1016/j.scitotenv.2017.01.138.